

Research Article

Open Access

Puja B. Chowdhury, Anirban Mitra, and Sarmila Sahoo*

Relative performance of antisymmetric angle-ply laminated stiffened hypar shell roofs with cutout in terms of static behavior

DOI 10.1515/cls-2016-0003

Received Nov 16, 2015; accepted Dec 02, 2015

Abstract: A review of literature reveals that bending analysis of laminated composite stiffened hypar shells with cutout have not received due attention. Being a doubly ruled surface, a skewed hypar shell fulfils aesthetic as well as ease of casting requirements. Further, this shell allows entry of north light making it suitable as civil engineering roofing units. Hypar shell with cutout subjected to uniformly distributed load exhibits improved performances with stiffeners. Hence relative performances of antisymmetric angle-ply laminated composite stiffened hypar shells in terms of displacements and stress resultants are studied in this paper under static loading. A curved quadratic isoparametric eight noded element and three noded beam elements are used to model the shell surface and the stiffeners respectively. Results obtained from the present study are compared with established ones to check the correctness of the present approach. A number of additional problems of antisymmetric angle-ply laminated composite stiffened hypar shells are solved for various fibre orientations, number of layers and boundary conditions. Results are interpreted from practical application standpoints and findings important for a designer to decide on the shell combination among a number of possible options are highlighted.

Keywords: stiffened hypar shell; cutout; antisymmetric angle ply composite; finite element method

1 Introduction

Hypar shells are used in civil engineering industry to cover large column free areas such as in stadiums, airports and


shopping malls. Being a doubly curved and doubly ruled surface, it satisfies aesthetic as well as ease of casting requirements of the industry. Moreover, hypar shell allows entry of daylight and natural air which is preferred in food processing and medicine units. Cutout is sometimes necessary in roof structure to allow entry of light, to provide accessibility of other parts of the structure, for venting and at times to alter the resonant frequency. Shell structure that are normally thin walled, when provided with cutout, exhibits improved performances with stiffeners. To use these doubly curved, doubly ruled surfaces efficiently, the behavior of these forms under bending are required to be understood comprehensively. The use of laminated composites to fabricate shells is preferred to civil engineers from second half of the last century. The reasons are high strength/stiffness to weight ratio, low cost of fabrication and better durability. Moreover, the stiffness of laminated composites can be altered by varying the fiber orientations and lamina thicknesses which gives designer flexibility. As a result, laminated shells are found more cost effective compared to the isotropic ones as application of laminated composites to fabricate shells reduces their mass induced seismic forces and foundation costs.

A thorough scrutiny of available literature on the bending behavior of laminated composite hypar shells with a cutout reveals that no study has been reported so far on this aspect. Sanders Jr. [1] and Ghosh and Bandyopadhyay [2] have considered the bending of isotropic shells with a cutout. The static behavior of a cylindrical composite panel in presence of cutouts has been reported using a geometrically non-linear theory [3] while the free vibration of cylindrical panel with square cutout has been studied based on finite element method [4]. The axisymmetric free vibration of isotropic shallow spherical shell with circular cutout has also been analyzed [5]. Madenci and Barut [6] studied buckling of composite panels in presence of cutouts. Non-linear post-buckling analysis of composite cylindrical panels with central circular cutouts but having no stiffeners was studied by Noor et al. [7] to consider the effect of edge shortening as well as uniform temperature change. Later Sai Ram and Babu [8, 9] investigated the bending behavior of axisymmetric composite spherical shell both punctured and un-punctured using the finite element method based on a higher order theory. Qatu

Puja B. Chowdhury: Department of Civil Engineering, Heritage Institute of Technology, Kolkata 700107, India

Anirban Mitra: Department of Mechanical Engineering, Jadavpur University, Kolkata 700032, India

***Corresponding Author: Sarmila Sahoo:** Department of Civil Engineering, Heritage Institute of Technology, Kolkata 700107, India, E-mail: sarmila.sahoo@gmail.com

 © 2015 P. B. Chowdhury et al., published by De Gruyter Open.

This work is licensed under the Creative Commons Attribution-NonCommercial-NoDerivs 3.0 License. The article is published with open access at www.degruyter.com.

et al. [10] reviewed the recent research studies on the static and buckling / post-buckling behavior of composite shells. Qatu et al. [11] reviewed the work done on the vibration aspects of composite shells between 2000-2009 and observed that most of the researchers dealt with closed cylindrical shells. Other shell geometries are also receiving considerable attention. Recently, Kumar et al. [12–15] considered finite element formulation for shell analysis using higher order zigzag theory. Vibration analysis of spherical shells and panels both shallow and deep has also been reported for different boundary conditions [16–19]. A complete and general view on mathematical modeling of laminated composite shells using higher order formulations has been provided in recent literature [20–22]. However, the bending behavior of antisymmetric angle-ply laminated composite stiffened hypar shell with cutout for various boundary conditions is scanty in the literature. Hence the objective of the present paper is to provide detailed information on bending behavior of these shell forms to evolve meaningful engineering design guidelines regarding choice of a particular shell option when a designer has to decide one among many such combinations. Since the overall suitability of a shell form can be concluded to some extent by giving due importance to static behavior, the present study takes a comprehensive approach to the problem.

2 Mathematical Formulation

2.1 Finite element formulation

A laminated composite hypar shell with cutout is shown in Figure 1. Differentiating the surface equation of shell in the form $z = f(x, y)$ yields the radius of cross curvature R_{xy} and for shallow shells considered in the present study the same is expressed as $\frac{1}{R_{xy}} = \frac{d^2z}{dx dy}$. An eight noded-curved quadratic isoparametric element (Figure 2) is used for the analysis of hypar shell. The five degrees of freedom taken into consideration at each node are u, v, w, α, β . The relations between the displacement at any point with respect to the co-ordinates ξ and η and the nodal degrees of freedom are expressed as:

$$\begin{aligned} u &= \sum_{i=1}^8 N_i u_i, & v &= \sum_{i=1}^8 N_i v_i, & w &= \sum_{i=1}^8 N_i w_i, \\ \alpha &= \sum_{i=1}^8 N_i \alpha_i, & \beta &= \sum_{i=1}^8 N_i \beta_i. \end{aligned} \quad (1)$$

In the isoparametric formulation the element geometry is also defined by the same shape functions, i.e.,

$$x = \sum_{i=1}^n N_i x_i, \quad y = \sum_{i=1}^n N_i y_i. \quad (2)$$

Here the shape functions are derived from a cubic interpolation polynomial and are given as:

$$\begin{aligned} N_i &= (1 + \xi \xi_i)(1 + \eta \eta_i)(\xi \xi_i + \eta \eta_i - 1)/4 & \text{for } i = 1, 2, 3, 4, \\ N_i &= (1 + \xi \xi_i)(1 - \eta^2)/2 & \text{for } i = 5, 7, \\ N_i &= (1 + \eta \eta_i)(1 - \xi^2)/2 & \text{for } i = 6, 8. \end{aligned} \quad (3)$$

The cubical shape functions $[N]$ adopted in the present study is same as those reported elsewhere [23]. The constitutive equations for the shell are given by (a list of notations is provided separately):

$$\{F\} = [D]\{\varepsilon\}, \quad (4)$$

where

$$\{F\} = \{N_x \ N_y \ N_{xy} \ M_x \ M_y \ M_{xy} \ Q_x \ Q_y\} \text{ (Figure 3)}$$

and

$$\{\varepsilon\} = \left\{ \varepsilon_x^0 \ \varepsilon_y^0 \ \gamma_{xy}^0 \ k_x \ k_y \ k_{xy} \ \gamma_{xz}^0 \ \gamma_{yz}^0 \right\}^T.$$

The laminate constitutive matrix $[D]$ and the finite element formulation for stiffeners used in the present study are adopted from Ref. [23].

The strain vector is related to the nodal values of element degree of freedoms by the strain displacement matrix $[B]$. The strain displacement matrix $[B]$ is also adopted from Ref. [23]. The strain-displacement relation is given by

$$\{\varepsilon\} = [B]\{d_e\}, \quad (5)$$

where

$$\{d_e\} = \{u_1 \ v_1 \ w_1 \ \alpha_1 \ \beta_1 \ \dots \ u_8 \ v_8 \ w_8 \ \alpha_8 \ \beta_8\}^T,$$

$$[B] = \sum_{i=1}^8 \begin{bmatrix} N_{i,x} & 0 & 0 & 0 & 0 \\ 0 & N_{i,y} & 0 & 0 & 0 \\ N_{i,y} & N_{i,x} & -2N_i/R_{xy} & 0 & 0 \\ 0 & 0 & 0 & N_{i,x} & 0 \\ 0 & 0 & 0 & 0 & N_{i,y} \\ 0 & 0 & 0 & N_{i,y} & N_{i,x} \\ 0 & 0 & N_{i,x} & N_i & 0 \\ 0 & 0 & N_{i,y} & 0 & N_i \end{bmatrix}.$$

Improved first order approximation theory for thin shell is used to establish the strain-displacement relations and the same are given as:

$$\begin{aligned} \{\varepsilon_x \ \varepsilon_y \ \gamma_{xy} \ \gamma_{xz} \ \gamma_{yz}\}^T &= \left\{ \varepsilon_x^0 \ \varepsilon_y^0 \ \gamma_{xy}^0 \ \gamma_{xz}^0 \ \gamma_{yz}^0 \right\}^T + \\ &+ z \{k_x \ k_y \ k_{xy} \ k_{xz} \ k_{yz}\}^T, \end{aligned} \quad (6)$$

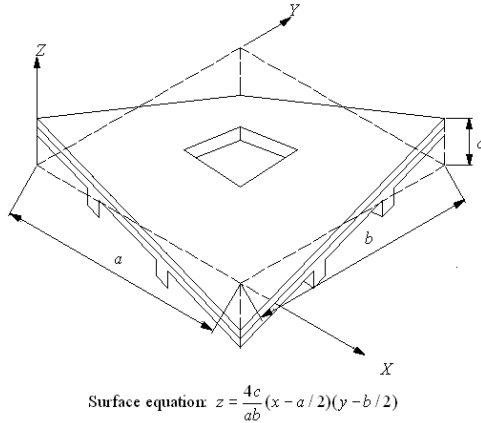


Figure 1: Surface of a skewed hyper shell with cutout

where

$$\begin{Bmatrix} \varepsilon_x^0 \\ \varepsilon_y^0 \\ \gamma_{xy}^0 \\ \gamma_{xz}^0 \\ \gamma_{yz}^0 \end{Bmatrix} = \begin{Bmatrix} \partial u / \partial x \\ \partial v / \partial y \\ \partial u / \partial y + \partial v / \partial x - 2w / R_{xy} \\ \alpha + \partial w / \partial x \\ \beta + \partial w / \partial y \end{Bmatrix}$$

and

$$\begin{Bmatrix} k_x \\ k_y \\ k_{xy} \\ k_{xz} \\ k_{yz} \end{Bmatrix} = \begin{Bmatrix} \partial \alpha / \partial x \\ \partial \beta / \partial y \\ \partial \alpha / \partial y + \partial \beta / \partial x \\ 0 \\ 0 \end{Bmatrix}.$$

In the above expression, the first vector denotes the mid-surface strain for a hyper shell and the second vector denotes the curvature.

The element stiffness matrix is

$$[K_{she}] = \iint [B]^T [D] [B] dx dy. \quad (7)$$

The two-dimensional integral is then converted to isoparametric coordinates and is evaluated by 2x2 Gauss-quadrature. This is because the shape functions are derived from a cubic interpolation polynomial and a polynomial of degree 2n-1 is integrated exactly by n point Gauss quadrature.

2.1.1 Finite Element Formulation for Stiffener of the Shell

The stiffeners are modeled using three noded curved isoparametric beam elements which are considered to run

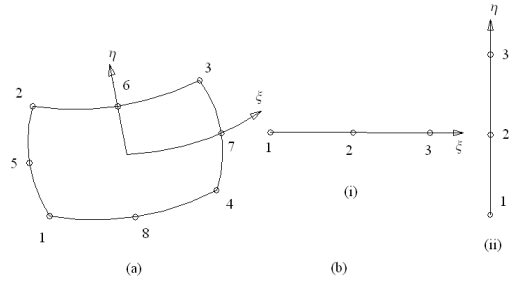


Figure 2: (a) Eight noded shell element with isoparametric coordinates (b) Three noded stiffener elements (i) x-stiffener (ii) y-stiffener

only along the boundaries of the shell elements. The shape functions of these beam elements for x and y directional stiffeners (shown in Figure 2) are as follows:

For x-stiffeners:

$$\begin{aligned} N_{\xi i} &= \xi \xi_i (1 + \xi \xi_i) & \text{for } i = 1, 3, \\ N_{\xi i} &= (1 - \xi^2) & \text{for } i = 2. \end{aligned} \quad (8)$$

For y-stiffeners:

$$\begin{aligned} N_{\eta i} &= \eta \eta_i (1 + \eta \eta_i) & \text{for } i = 1, 3, \\ N_{\eta i} &= (1 - \eta^2) & \text{for } i = 2. \end{aligned} \quad (9)$$

In the stiffener element, each node has four degrees of freedom i.e. u_{sx} , w_{sx} , α_{sx} and β_{sx} for x-stiffener and u_{sy} , w_{sy} , α_{sy} and β_{sy} for y-stiffener. The displacement field at any point can be expressed in terms of nodal displacements as follows:

$$\begin{aligned} \text{for x-stiffener: } \{\delta_{sx}\} &= [N_{\xi i}] \{\delta_{sxi}\}, \\ \text{for y-stiffener: } \{\delta_{sy}\} &= [N_{\eta i}] \{\delta_{syi}\}, \end{aligned} \quad (10)$$

where

$$\begin{aligned} \{\delta_{sxi}\} &= [u_{sx1} \ w_{sx1} \ \alpha_{sx1} \ \beta_{sx1} \ \dots \ u_{sx3} \ w_{sx3} \ \alpha_{sx3} \ \beta_{sx3}]^T, \\ \{\delta_{syi}\} &= [v_{sy1} \ w_{sy1} \ \alpha_{sy1} \ \beta_{sy1} \ \dots \ v_{sy3} \ w_{sy3} \ \alpha_{sy3} \ \beta_{sy3}]^T. \end{aligned}$$

The generalized force-displacement relation of stiffeners can be expressed as:

$$\begin{aligned} \text{for x-stiffener: } \{F_{sx}\} &= [D_{sx}] \{\varepsilon_{sx}\} = [D_{sx}] \{B_{sx}\} \{\delta_{sxi}\}, \\ \text{for y-stiffener: } \{F_{sy}\} &= [D_{sy}] \{\varepsilon_{sy}\} = [D_{sy}] \{B_{sy}\} \{\delta_{syi}\}, \end{aligned} \quad (11)$$

where

$$\begin{aligned} \{F_{sx}\} &= [N_{sxx} \ M_{sxx} \ T_{sxx} \ Q_{sxxx}]^T, \\ \{\varepsilon_{sx}\} &= [u_{sx,x} \ \alpha_{sx,x} \ \beta_{sx,x} \ (\alpha_{sx} + w_{sx,x})]^T \end{aligned}$$

and

$$\{F_{sy}\} = [N_{syy} \ M_{syy} \ T_{syy} \ Q_{syyz}]^T,$$

$$\{\varepsilon_{sy}\} = [v_{sy,y} \ \beta_{sy,y} \ \alpha_{sy,y} \ (\beta_{sy} + w_{sy,y})]^T.$$

Elasticity matrices are as follows:

$$[D_{sx}] =$$

$$= \begin{bmatrix} A_{11}b_{sx} & B'_{11}b_{sx} & B'_{12}b_{sx} & 0 \\ B'_{11}b_{sx} & D'_{11}b_{sx} & D'_{12}b_{sx} & 0 \\ B'_{12}b_{sx} & D'_{12}b_{sx} & \frac{1}{6}(Q_{44} + Q_{66})d_{sx}b_{sx}^3 & 0 \\ 0 & 0 & 0 & b_{sx}S_{11} \end{bmatrix}$$

and

$$[D_{sy}] =$$

$$= \begin{bmatrix} A_{22}b_{sy} & B'_{22}b_{sy} & B'_{12}b_{sy} & 0 \\ B'_{22}b_{sy} & \frac{1}{6}(Q_{44} + Q_{66})b_{sy} & D'_{12}b_{sy} & 0 \\ B'_{12}b_{sy} & D'_{12}b_{sy} & D'_{11}d_{sy}b_{sy}^3 & 0 \\ 0 & 0 & 0 & b_{sy}S_{22} \end{bmatrix},$$

where

$$D'_{ij} = D_{ij} + 2eB_{ij} + e^2A_{ij},$$

$$B'_{ij} = B_{ij} + eA_{ij}. \quad (12)$$

A_{ij} , B_{ij} , D_{ij} and S_{ij} are the stiffness coefficients. Here the shear correction factor is taken as 5/6. The sectional parameters are calculated with respect to the mid-surface of the shell by which the effects of eccentricity of the x-stiffener, e_{sx} and y-stiffener, e_{sy} are automatically included. The element stiffness matrix:

$$\text{for x-stiffener: } [K_{xe}] = \int [B_{sx}]^T [D_{sx}] [B_{sx}] dx,$$

$$\text{for y-stiffener: } [K_{ye}] = \int [B_{sy}]^T [D_{sy}] [B_{sy}] dy. \quad (13)$$

The integrals are then converted to isoparametric coordinates and are evaluated by 2 point Gaussian quadrature.

2.1.2 Solution Procedure

Finally, appropriate matching of the nodes of the stiffener and shell elements through the connectivity matrix yields the element stiffness matrix of the stiffened shell and the same is given as:

$$[K_e] = [K_{she}] + [K_{xe}] + [K_{ye}]. \quad (14)$$

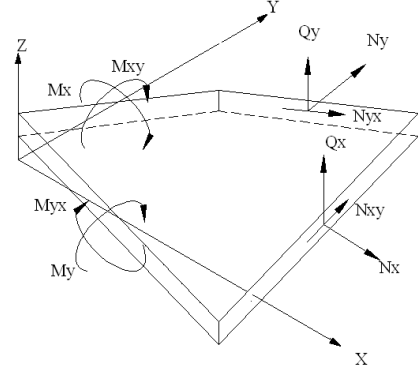


Figure 3: Generalized force and moment resultants

The global stiffness matrices are obtained by assembling the element stiffness matrices. The global load vector $\{P\}$ is formed by incorporating the magnitude of the transverse point load corresponding to the appropriate degree of freedom at the node where it is applied. The basic static problem takes the form:

$$[K]\{d\} = \{P\}, \quad (15)$$

where $[K]$ is the overall stiffness matrix, $\{d\}$ and $\{P\}$ are generalized displacement and load vectors, respectively. After imposing the boundary conditions, the Gauss elimination technique is used to solve the above equation that yields the global nodal displacement vector $\{d\}$. Hence the element displacement vectors $\{d_e\}$ are known. Using $\{d_e\}$ in Equation (5) the strains can be evaluated at the Gauss points, which when used in Equation (4) the generalized force and moment resultants are obtained at the Gauss points. Extrapolation of these values yields the nodal values.

2.2 Modeling the cutout

The code developed has the provision to incorporate the position and size of cutout as input. The program is capable of generating non uniform finite element mesh all over the shell surface. So the element size is gradually decreased near the cutout margins. One such typical non-uniform mesh arrangement is shown in Figure 4.

3 Numerical Problems

To establish the correctness of the static formulations of the finite element code proposed in this paper, for the

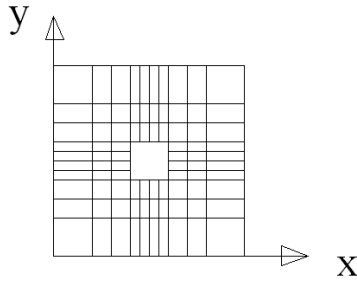


Figure 4: Typical 10x10 non-uniform mesh arrangements drawn to scale

analysis of stiffened shell the authors compared their results with pre-established results reported by Rossow and Ibrahimkhail [24] using constrained method of finite element analysis, by Chang [25] using conventional method of analysis, by Sinha *et al.* [26] and also by using structural packages NASTRAN, STRUDL. Static displacements of simply supported plates are evaluated using the present formulation and a comparison of central displacements obtained by different methods is presented in Table 1. The material and geometric properties of the plates are presented with the table as footnote. In order to solve a plate problem with the present formulation, the corner rise of the hypar (c) is made zero. Present composite shell formulation is used for the isotropic material by making the elastic and shear moduli equal in all directions.

To validate the cutout formulation of the present code, the authors solve additional problem as benchmark. The second problem was solved earlier by Chakravorty *et al.* [27] and deals with free vibration of hypar shell with cutouts having simply supported and clamped boundary conditions. The relevant parameters are furnished with Table 2 showing the correctness of the cutout formulation. The finite element mesh is refined in steps and a particular grid is chosen to obtain the fundamental frequency when the result does not improve by more than one percent on further refining. Convergence of results is ensured in all the problems taken up here.

Apart from the benchmark problems, the authors solve additional problems of static responses of graphite-epoxy multilayered composite hypar shells. Antisymmetric angle ply stacking sequences and different boundary conditions (Figure 5) are considered. The non-dimensional values of static displacements, static stress resultants of different shell combinations are presented systematically in Table 3 to Table 15. The material and geometric properties of the hypar shells for additional problems are con-

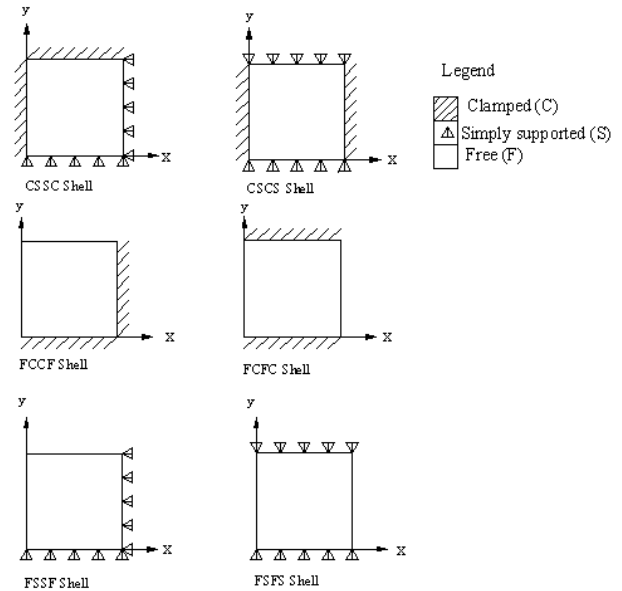


Figure 5: Arrangement of boundary conditions

sidered as: $a/b = 1$, $a'/b' = 1$, $a/h = 100$, $c/a = 0.2$, $E_{11} = 25E_{22}$, $G_{12} = G_{13} = 0.5E_{22}$, $G_{23} = 0.2E_{22}$, $\nu = 0.25$, $\rho = 100 \text{ N-sec}^2/\text{m}^4$.

4 Results and Discussion

4.1 Benchmark problems

Table 1 and Table 2 show very good agreement of the present results with the established ones and this validate the static formulation of stiffened hypar shell with cutout. Table 2 also shows the convergence of fundamental frequencies with increasingly finer mesh and an 10x10 division is taken up for further study since the values do not improve by more than 1% on further refining. Close agreement of present results with benchmark ones establishes the fact that the finite element model proposed here is capable of analyzing static problems of stiffened skewed hypar composite shells with cutout.

4.2 Additional problems

Non-dimensional static displacements and stress resultants of composite stiffened hypar shell with cutouts are presented in Table 3 to Table 15 for different antisymmetric angle ply stacking sequences of graphite-epoxy composite with six different boundary conditions. Orthotropic shells

Table 1: Central deflection of rectangular stiffened plate in inches ($\times 10^3$).

Source	Concentrated Load		Distributed Load	
	Eccentric	Concentric	Eccentric	Concentric
Rossow and Ibrahimkhail [24]	1.270	3.464	8.850	24.075
Chang [25]	1.246	3.464	8.996	24.077
NASTRAN	1.240	-	8.714	-
STRUDL	-	3.463	-	24.120
Sinha et al.[26]	1.284	3.464	9.322	24.075
Present method	1.313	3.492	8.905	24.011

$E=30 \times 10^6$ psi; $\nu = 0.3$; $a=30$ in; $b=60$ in; $h=0.25$ in; x-stiffener 0.5×5.0 in²; y-stiffener 0.5×3.0 in².

Table 2: Non-dimensional fundamental frequencies ($\bar{\omega}$) for hypar shells (lamination $(0/90)_4$) with concentric cutouts.

a'/a	Chakravorty et al. [27]		Present finite element model					
	Simply supported	clamped	Simply supported			clamped		
			8x8	10x10	12x12	8x8	10x10	12x12
0.0	50.829	111.600	50.573	50.821	50.825	111.445	111.592	111.612
0.1	50.769	110.166	50.679	50.758	50.779	109.987	110.057	110.233
0.2	50.434	105.464	50.323	50.421	50.400	105.265	105.444	105.443
0.3	49.165	101.350	49.045	49.157	49.178	101.110	101.340	101.490
0.4	47.244	97.987	47.132	47.242	47.141	97.670	97.985	97.991

$a/b = 1$, $a/h = 100$, $a'/b' = 1$, $c/a = 0.2$; $E_{11}/E_{22} = 25$, $G_{23} = 0.2E_{22}$, $G_{13} = G_{12} = 0.5E_{22}$, $\nu_{12} = \nu_{21} = 0.25$.

$(0^\circ, 90^\circ)$ are also included to study the variation of deflection and stress resultants with change in lamination angle. Governing static force and moment resultants (including the deflection, in-plane forces and bending moments which govern the shell thickness) are presented. Performances of the shell combinations in terms of their stress resultants are ranked from 1 to 6. For ranking, only the antisymmetric angle ply stacking sequences are considered. The first rank is given to the shell combination showing least static stress resultant value. Such ranks are very helpful to understand the relative behavior of shell options comprehensively.

4.2.1 Effect of boundary conditions on relative performance of composite stiffened hypar shells with cutouts

Close observation in terms of static deflections from Table 3 reveal that Group III shells show lower values when compared to Group I shells for any given lamination. This is quite obvious as in Group I boundary condition, increased number of boundary restraints restrict its possible movements along the boundaries and makes the shell stiffer compared to Group II ones which in turn exhibit lesser de-

flections than Group III shell, where more number of support degrees of freedom are released. But it is further noted from Table 3 that when a free edge is introduced into a shell maximum deflection occurs along the free edges otherwise maximum deflection occur along the periphery of the cutout.

It is further noted from Table 3 that deflection increases significantly when a Group IA shell is replaced by a Group IIA shell. However, if a Group IIA shell is replaced by a Group IIIA shell the deflection increases marginally and at times by an insignificant amount. The same trend is noticeable for Group IB, Group IIB and Group IIB shell as well. If Group IB shell is replaced by a Group IIB shell, deflection significantly increases but when a Group IIB shell is replaced by a Group IIIB shell the increase in deflection is not so significant.

A close observation of the results for Group I boundary conditions reveals that the CSSC shells are superior in performance showing lesser deflections than CSCS shells for the antisymmetric angle ply laminates having lamination angle upto 45° . But reverse is the case for lamination angles greater than 45° where CSCS edge shows higher static stiffness than CSSC edge. Thus CSCS shells are better choices than CSSC ones for higher lamination angles.

It is further noted that shells of Group I having CSSC

and CSCS boundaries have comparable maximum deflection. But in case of Group II and Group III shells a change in the arrangement of boundary constraints has huge impact on static stiffness. When two opposite free edges are introduced in a shell, it is far stiffer than a shell for which two adjacent edges are free. As a result FCFC and FSFS shells show less deflection than FCCF and FSSF shells. This is true for all laminations except 45° lamination angle, where reverse trend is observed. Thus while keeping the number of support constraints fixed, a change of arrangement of the conditions of individual edges involving free edges markedly influences the maximum deflection.

Comparative study of governing static stress resultants shows that performance of Group I shells is not at all comparable with other groups (Group II and Group III) for in-plane forces and in-plane shear. Only for a few cases in-plane force and in-plane shear shows comparable values. But for sagging, hogging and twisting moment resultants, although Group I shells show lower value than Group II and Group III shells, again a very few exception is there. These findings reinforce the fact that in composite shells, lamination angle plays a very important role along with the support condition to determine resultant stiffness. It is also evident that relative performance study of shells in terms of their deflections cannot be taken as the only basis of comparing their overall performance. A closed scrutiny of the results also reveals that, Group I shells exhibit maximum static stress resultants around the cutout but Group II and Group III shells show towards the free edges.

4.2.2 Relative performance of composite stiffened hyper shells with cutout for different lamination angles

In civil engineering applications among two shell forms the one which exhibits lower deflection is accepted as a better option from serviceability point of view. It is evident from Table 3 that, for a given number of boundary constraints, $(+45/-45)_5$ antisymmetric laminate is the best choice. Also number of lamina plays an important role in static deflection consideration. In all the cases considered here, 10 layer antisymmetric laminates are convincingly better than four layer and two layer angle ply ones. It is interesting to note from Tables 4–15, that for all the boundary conditions for any two laminations the one which performs better in terms of deflection is not better in terms of other static stress resultants. For static stress resultants like $+\bar{N}_x$, $-\bar{N}_x$, $-\bar{M}_x$ lower lamination angle and for $+\bar{N}_y$, $-\bar{N}_y$, $-\bar{M}_y$ higher lamination angle is better choices but for other shell actions however, such unified behavior is not found to hold good.

Results of Table 3 to Table 15 show that in general 10 layer laminates exhibit better performance compared to two and four layered ones in terms of static deflections and static stress resultants with a few exception where 4 layer laminates are better than 10 layer laminates.

4.2.3 Performances of Different Boundary Conditions with respect to different Shell Actions

Now an attempt is made in the present study of antisymmetric angle ply laminates to compare the relative performance of boundary conditions. For each shell action, the best two combinations of lamination and edge condition are selected from each of three groups of boundary conditions. Thus total six combinations are selected from three Groups. These have been furnished in Table 16 and Table 17 for positive and negative values of shell actions in ascending order of magnitude. For example, the CSCS/(30/-30) shell is the best choice for both positive and negative \bar{N}_x while CSCS/(75/-75) shell is the best choice for both positive and negative \bar{N}_y . This rank wise arrangement of the shells in terms of lamination along with boundary condition corresponding to the different shell actions will help a design engineer to make a choice among a number of options when it is known that which shell action is critical for a particular situation. It is noteworthy to mention here that superiority of a particular shell combination expressed in terms of lamination and boundary conditions for one particular shell action cannot be used as the guideline of predicting the relative performances for other shell actions.

Based on the results available in Tables 3–15, it is possible to develop a relative performance matrix of the shells so as to help a design engineer to conclusively decide upon the selection among two different combinations of laminations and boundary conditions. The relative performance matrix of the shells may be developed in the following way. Among two choices of lamination and edge condition, the superior combination is assigned a value of 1 while the inferior combination is assigned 0 with respect to different shell actions. If two combinations show almost equal values of a particular shell action, the number 1 may be assigned to both of them. One such typical performance matrix is shown in Table 18 comparing CSCS/(15/-15)₂ and CSCS/(45/-45)₂ shells. A design engineer can now take a conclusive decision for choice between two shells applying appropriate weightage factors to the different shell actions if such relative performance matrix is made available.

5 Conclusions

Following conclusions can be drawn from the present study,

1. The close agreement between the results obtained by the present approach and those appearing in the published literature establishes the correctness of the formulation.
2. An increase in support restraints always reduces the deflection and static stress resultants near the boundary.
3. Among shells with two boundaries clamped and other two simply supported, the ones with adjacent boundaries clamped show lesser deflection for all the antisymmetric laminations considered here.
4. Among shells with two free boundaries, one with two adjacent boundaries free shows greater static deflection for all the antisymmetric laminations considered here.
5. Free boundaries bring in higher flexibility in shells and in this respect whether the other boundaries are simply supported or clamped matters to a great extent. Also when a free boundary is introduced to a stiffened shell with cutout, maximum deflection and stress resultants always occur near the free boundary.
6. The superiority of a particular combination in terms of a shell action cannot predict the performance of the shell for other shell actions.

Notations

a, b - length and width of shell in plan
 a', b' - length and width of cutout in plan
 b_{sx}, b_{sy} - width of x and y stiffener respectively
 c - rise of hypar shell
 $\{d\}$ - global displacement vector
 d_{st} - depth of stiffener
 d_{sx}, d_{sy} - depth of x and y stiffener respectively
 $\{d_e\}$ - element displacement
 D - flexural rigidity
 e_{sx}, e_{sy} - eccentricities of x and y stiffeners with respect to mid surface of shell
 E_{11}, E_{22} - elastic moduli
 G_{12}, G_{13}, G_{23} - shear moduli of a lamina with respect to 1, 2 and 3 axes of fibre
 h - shell thickness
 M_x, M_y - moment resultants
 M_{sxx}, M_{syy} - moment resultants of stiffener
 M_{xy} - torsion resultant
 \bar{M}_x, \bar{M}_y - non-dimensional moment resultant
 $[= (M_x \text{ or } M_y)/qa^2]$

\bar{M}_{xy} - non-dimensional torsion resultant
 $[= M_{xy}/qab]$
 np - number of plies in a laminate
 $N_1 - N_8$ - shape functions
 N_x, N_y - in-plane force resultants
 N_{sxx}, N_{syy} - axial force resultants of stiffeners
 N_{xy} - in-plane shear resultant
 \bar{N}_x, \bar{N}_y - non-dimensional in-plane force resultants
 $[= (N_x \text{ or } N_y)/qa]$
 \bar{N}_{xy} - non-dimensional in-plane shear resultant $[= N_{xy}/qa]$
 Q_x, Q_y - transverse shear resultants
 Q_{sxxz}, Q_{syyz} - transverse shear resultants of stiffener
 q - intensity of uniformly distributed transverse load
 R_{xy} - radii of cross curvature of hypar shell
 T_{sxx}, T_{syy} - torsion resultants of stiffeners
 u, v, w - translational degrees of freedom at each node of shell element
 w_{st} - width of stiffener
 u_{sx}, w_{sx} - translational degrees of freedom at each node of x-stiffener element
 v_{sy}, w_{sy} - translational degrees of freedom at each node of y-stiffener element
 x, y, z - local co-ordinate axes
 X, Y, Z - global co-ordinate axes
 \bar{x} - non-dimensional x co-ordinate $[= x/a]$
 \bar{y} - non-dimensional y co-ordinate $[= y/b]$
 z_k - distance of bottom of the kth ply from mid-surface of a laminate
 α, β - rotational degrees of freedom at each node of shell element
 α_{sx}, β_{sx} - rotational degrees of freedom at each node of x-stiffener element
 α_{sy}, β_{sy} - rotational degrees of freedom at each node of y-stiffener element
 ϵ_x, ϵ_y - in-plane strain component
 $\gamma_{xy}, \gamma_{xz}, \gamma_{yz}$ - shearing strain components
 ν_{12}, ν_{21} - Poisson's ratios
 ξ, η, τ - isoparametric co-ordinates
 ρ - density of material
 σ_x, σ_y - in-plane stress components
 $\tau_{xy}, \tau_{xz}, \tau_{yz}$ - shearing stress components
 ω - natural frequency
 $\bar{\omega}$ - non-dimensional natural frequency
 $[= \omega a^2 (\rho/E_{11} h^2)^{1/2}]$

References

- [1] Sanders Jr. J.L., Cutouts in Shallow shells, *J. Appl. Mech.*, 1970, 37, 374-383.
- [2] Ghosh B., Bandyopadhyay J.N., Bending analysis of conical shells with cutouts. *Computers & Structures*, 1994, 53, 9-18.
- [3] Dennis S.T., Palazotto A.N., Static response of a cylindrical composite panel with cutouts using a geometrically nonlinear theory, *AIAA J*, 1990, 28, 1082-1108.
- [4] Sivasubramanian B., Kulkarni A.M., Venkateswara Rao G., Free vibration of curved panels with cutouts. *J. Sound Vib.* 1997, 200, 227-234.
- [5] Hwang D.Y., Foster Jr. W.A., Analysis of axisymmetric free vibration of isotropic shallow spherical shells with a circular hole, *J. Sound Vib.* 1992, 157, 331-343.
- [6] Madenci E., Barut A., Pre and post-buckling response of curved thin composite panels with cutouts under compression, *Int J Numer Meth Engrg*, 1994, 37, 1499-1510.
- [7] Noor A.K., Starnes J.H., Peters J.M., Nonlinear and postbuckling responses of curved composite panels with cutouts, *Composite Structures*, 1996, 34, 213-240.
- [8] Sai Ram K.S., Babu T.S., Study of bending of laminated composite shells, Part I: shells without a Cutout, *Composite Structures*, 51(1), 2001, 103-116.
- [9] Sai Ram K.S., Babu T.S., Study of bending of laminated composite shells, Part II: shells with a Cutout, *Composite Structures*, 51(1), 2001, 117-126.
- [10] Qatu M.S., Asadi E., Wang W., Review of recent literature on static analyses of composite shells: 2000-2010, *Open Journal of Composite Materials*, 2012, 2, 61-86.
- [11] Qatu M.S., Sullivan R. W., Wang W., Recent research advances on the dynamic analysis of composite shells:2000-2009, *Composite Structures*, 2010, 93, 14-31.
- [12] Kumar A., Chakrabarti A., Bhargava P., Finite element analysis of laminated composite and sandwich shells using higher order zigzag theory, *Composite Structures*, 2013, 106, 270-281.
- [13] Kumar A., Chakrabarti A., Bhargava P., Vibration of laminated composites and sandwich shells based on higher order zigzag theory, *Engineering Structures*, 2013, 56, 880-888.
- [14] Kumar A., Chakrabarti A., Bhargava P., Vibration of laminated composite shells with cutouts using higher order shear deformation theory, *International Journal of Scientific & Engineering Research*, 2013, 4(5), 199-202.
- [15] Kumar A., Chakrabarti A., Bhargava P., Accurate dynamic response of laminated composites and sandwich shells using higher order zigzag theory, *Thin Walled Structures*, 2014, 77, 174-186.
- [16] Ye T., Jin G., Chen Y., Ma X., Su Z., Free vibration analysis of laminated composite shallow shells with general elastic boundaries, *Composite Structures*, 2013, 106, 470-490.
- [17] Ye T., Jin G., Chen Y., Shi S., A unified formulation for vibration analysis of open shells with arbitrary boundary conditions, *International Journal of Mechanical Sciences*, 2014, 81, 42-59.
- [18] Jin G., Ye T., Jia X., Gao S., A general Fourier solution for the vibration analysis of composite laminated structure elements of revolution with general elastic restraints, *Composite Structures*, 2014, 109, 150-168.
- [19] Ye T., Jin G., Su Z., Jia X., A unified Chebyshev-Ritz formulation for vibration analysis of composite laminated deep open shells with arbitrary boundary conditions, *Arch. Appl. Mech.*, 2014, 84, 441-471.
- [20] Tornabene F., Fantuzzi N., Bacciocchi M., The local GDQ method applied to general higher-order theories of doubly-curved laminated composite shells and panels: the free vibration analysis, *Composite Structures*, 2014, 116, 637-660.
- [21] Tornabene F., Fantuzzi N., Viola E., Reddy J.N., Winkler-Pasternak foundation effect on the static and dynamic analyses of laminated doubly-curved and degenerate shells and panels, *Composites Part B Engineering*, 2014, 57(1), 269-296.
- [22] Tornabene F., Viola E., Fantuzzi N., General higher-order equivalent single layer theory for free vibrations of doubly-curved laminated composite shells and panels, *Composite Structures*, 2013, 104(1), 94-117.
- [23] Sahoo S., Chakravorty, D., Deflections, forces and moments of composite stiffened hypar shell roofs under concentrated load, *Journal of Strain Analysis for Engineering Design*, 2006, 41(1), 81-97.
- [24] Rossow, M. P., Ibrahimkhail, A.K., Constrained method analysis of stiffened plates, *Computers & Structures*, 1978, 8, 51-60.
- [25] Chang, S.P., Analysis of eccentrically stiffened plates, Ph. D. Thesis, University of Missouri, Columbia, MO, 1973.
- [26] Sinha, G., Sheikh, A H., Mukhopadhyay, M., A new finite element model for the analysis of arbitrary stiffened shells, *Finite Elements in Analysis and Design*, 1992, 12, 241-271.
- [27] Chakravorty D., Sinha P.K., Bandyopadhyay J.N., Applications of FEM on free and forced vibration of laminated shells, *ASCE Journal of Engineering Mechanics*, 1998; 124(1), 1-8.

Table 3: Values of maximum non-dimensional downward deflections ($-\bar{w}$) $\times 10^4$ for different antisymmetric angle ply lamination and boundary conditions of stiffened composite hypar shell with cutout.

Lamination (Degree)	Boundary conditions					
	Group-I		Group-II		Group-III	
	A CSSC	B CSCS	A FCCF	B FCFC	A FSSF	B FSFS
0	-1.3281 (0.55,0.4)	-1.4671 (0.5,0.6)	-5.3354 (0.5,1.0)	-1.983 (0.0,0.5)	-5.8823 (0.3,1.0)	-2.0482 (0.0,0.5)
(15/-15)	-0.51441 (0.5,0.4)	-0.57554 (0.5,0.4)	-5.7156 (0.7,1.0)	-1.0488 (0.0,0.5)*	-6.2017 (0.3,1.0)	-1.2776 (0.0,0.5)
(15/-15) ₂	-0.4655 (0.5,0.4)	-0.52171 (0.5,0.4)	-4.432 (0.5,1.0)	-1.0504 (0.0,0.5)	-4.6521 (0.5,1.0)	-1.1396 (0.0,0.5)
(15/-15) ₅	-0.4495 (0.6,0.45)	-0.50187 (0.5,0.4)	-4.1361 (0.5,1.0)	-1.0614 (0.0,0.5)	-4.2423 (0.5,1.0)	-1.1062 (1.0,0.5)*
(30/-30)	-0.27818 (0.6,0.5)	-0.2863 (0.5,0.6)	-4.1111 (0.7,1.0)	-1.3301 (1.0,0.5)	-4.3846 (0.3,1.0)	-1.4903 (1.0,0.5)
(30/-30) ₂	-0.2363 (0.6,0.5)	-0.24699 (0.5,0.6)	-3.2274 (0.5,1.0)	-1.2836 (0.0,0.5)*	-3.3642 (0.5,1.0)	-1.3477 (1.0,0.5)
(30/30) ₅	-0.22063 (0.6,0.5)	-0.2314 (0.5,0.4)	-3.0679 (0.5,1.0)	-1.2895 (0.0,0.5)	-3.1243 (0.5,1.0)	-1.3188 (1.0,0.5)*
(45/-45)	-0.24886 (0.6,0.5)	-0.21628 (0.5,0.6)	-2.4562 (0.0,0.7)	-2.5173 (1.0,0.7)	-3.0157 (0.0,0.7)	-2.6592 (1.0,0.5)
(45/-45) ₂	-0.20478 (0.6,0.5)	-0.19012 (0.5,0.6)	-2.0948 (0.0,0.5)	-2.2666 (1.0,0.5)	-2.3205 (0.0,0.55)	-2.3752 (1.0,0.5)
(45/-45) ₅	-0.18956 (0.6,0.5)	-0.17932 (0.5,0.6)*	-2.0522 (0.0,0.5)	-2.222 (0.0,0.5)	-2.216 (0.0,0.5)	-2.3097 (1.0,0.5)
(60/-60)	-0.28683 (0.6,0.5)	-0.24931 (0.4,0.5)	-4.2754 (0.0,0.3)	-3.9971 (0.0,0.3)	-4.5769 (0.0,0.7)	-4.122 (1.0,0.3)
(60/-60) ₂	-0.24535 (0.6,0.5)	-0.22869 (0.5,0.4)	-3.3999 (0.0,0.5)	-3.196 (0.0,0.3)	-3.5752 (0.0,0.5)	-3.5268 (0.0,0.5)
(60/-60) ₅	-0.23117 (0.6,0.5)	-0.2197 (0.5,0.6)*	-3.2451 (0.0,0.5)	-3.0483 (0.0,0.5)	-3.3441 (0.0,0.5)	3.3852 (1.0,0.5)
(75/-75)	-0.53 (0.6,0.5)	-0.49 (0.6,0.5)	-5.72 (0.0,0.3)	-5.21 (1.0,0.3)	-6.20 (0.0,0.7)	-5.54 (1.0,0.3)
(75/-75) ₂	-0.48 (0.6,0.5)	-0.47 (0.5,0.6)	-4.54 (0.0,0.5)	-4.04 (0.0,0.3)	-4.79 (0.0,0.5)	-4.64 (1.0,0.5)
(75/-75) ₅	-0.47 (0.6,0.5)	-0.46 (0.5,0.6)	-4.24 (0.0,0.5)	-3.70 (1.0,0.3)	-4.39 (0.0,0.5)	-4.39 (1.0,0.5)
90	-1.361 (0.6,0.45)	-1.2916 (0.5,0.6)	-5.3926 (0.0,0.5)	-4.6674 (0.0,0.7)	-5.9227 (0.0,0.65)	-5.4571 (0.0,0.5)

$a/b = 1, a/h = 100, a'/b' = 1, c/a = 0.2; E_{11}/E_{22} = 25, G_{23} = 0.2E_{22}, G_{13} = G_{12} = 0.5E_{22}, \nu_{12} = \nu_{21} = 0.25.$

Values in the parenthesis indicates the location (\bar{x}, \bar{y}) of maximum downward deflection in each case.

Asterisk denotes the lowest values of shell actions in each group.

Table 4: Values of maximum non-dimensional tensile in-plane forces ($+\bar{N}_x$) for different antisymmetric angle ply lamination and boundary conditions of stiffened composite hyarp shell with cutout

Lamination (Degree)	Boundary conditions					
	Group-I		Group-II		Group-III	
	A CSSC	B CSCS	A FCCF	B FCFC	A FSSF	B FSFS
0	0.31957 (0.0,0.8)	0.23068 (0.6,0.6)	7.6766 (0.0,1.0)	0.072831 (0.3,0.3)	9.7331 (0.0,1.0)	0.42598 (0.0,0.9)
(15/-15)	0.33909 (0.0,0.9)	0.21061 (1.0,0.1)	8.4345 (0.0,1.0)	0.40015 (0.0, 1.0)*	9.2218 (0.0,1.0)	1.0713 (0.0, 1.0)*
(15/-15) ₂	0.28265 (0.0,0.9)	0.19707 (0.6, 0.6)*	8.2291 (0.0,1.0)	0.4439 (1.0,0.0)	9.2332 (0.0,1.0)	1.0882 (1.0,0.0)
(15/-15) ₅	0.25797 (0.0,0.9)	0.20857 (0.4,0.4)	8.1402 (0.0,1.0)	0.46501 (0.0,1.0)	9.2351 (0.0,1.0)	1.1021 (0.0,1.0)
(30/-30)	0.34845 (0.0,0.9)	0.19052 (0.6, 0.6)*	9.1489 (0.0,1.0)	1.9587 (0.0,1.0)	9.3434 (0.0,1.0)	4.1624 (0.0, 1.0)*
(30/-30) ₂	0.32936 (0.0,0.9)	0.21 (0.6,0.6)	8.9634 (0.0,1.0)	1.9095 (0.0,1.0)	9.3717 (0.0,1.0)	4.2145 (0.0,1.0)
(30/30) ₅	0.32108 (0.0,0.9)	0.21675 (0.6,0.6)	8.9018 (0.0,1.0)	1.9193 (0.0,1.0)	9.3868 (0.0,1.0)	4.2466 (0.0,1.0)
(45/-45)	0.62534 (1.0,0.0)	0.32589 (0.4,0.4)	10.702 (0.0,1.0)	5.2897 (1.0,0.0)	10.908 (0.0,1.0)	9.6308 (1.0,0.0)
(45/-45) ₂	0.45906 (0.0,0.9)	0.31976 (0.6,0.6)	10.498 (0.0,1.0)	4.8639 (0.0,1.0)	10.922 (0.0,1.0)	9.9459 (0.0,1.0)
(45/-45) ₅	0.45662 (0.0,0.9)	0.31743 (0.6,0,,6)	10.431 (0.0,1.0)	4.7968 (0.0,1.0)	10.94 (0.0,1.0)	10.058 (0.0,1.0)
(60/-60)	0.73981 (0.0,0.9)	0.5485 (0.6,0.6)	12.519 (0.0,1.0)	6.9077 (0.0,1.0)	13.657 (0.0,1.0)	15.74 (0.0,1.0)
(60/-60) ₂	0.74688 (0.0,0.9)	0.52605 (0.6,0.6)	11.802 (0.0,1.0)	5.956 (0.0,1.0)	13.333 (0.0,1.0)	16.843 (0.0,1.0)
(60/-60) ₅	0.74834 (0.0,0.9)	0.5145 (0.6,0.6)	11.641 (0.0,1.0)	5.7328 (0.0,1.0)	13.298 (0.0,1.0)	17.207 (0.0,1.0)
(75/-75)	1.0767 (0.0,0.9)	0.86053 (0.6,0.6)	10.221 (0.0,1.0)	2.5636 (1.0,0.0)	13.999 (0.0,1.0)	4.9594 (0.0,1.0)
(75/-75) ₂	1.0893 (0.0,0.9)	0.81437 (0.6,0.6)	9.312 (0.0,1.0)	1.9671 (0.0,1.0)	13.2 (0.0,1.0)	4.4089 (0.0,1.0)
(75/-75) ₅	1.1045 (0.0,0.9)	0.79251 (0.6,0.6)	9.1627 (0.0,1.0)	1.7865 (0.0, 1.0)*	13.117 (0.0,1.0)	4.3593 (0.0,1.0)
90	1.5768 (0.0,0.0)	1.3692 (1.0,1.0)	5.5273 (0.0,1.0)	1.2854 (0.35,0.4)	16.167 (0.0,0.0)	15.315 (0.0,0.0)

$a/b = 1$, $a/h = 100$, $a'/b' = 1$, $c/a = 0.2$; $E_{11}/E_{22} = 25$, $G_{23} = 0.2E_{22}$, $G_{13} = G_{12} = 0.5E_{22}$, $\nu_{12} = \nu_{21} = 0.25$.

Values in the parenthesis indicates the location (\bar{x}, \bar{y}) of maximum tensile in-plane force in each case.

Asterisk denotes the lowest values of shell actions in each group.

Table 5: Values of maximum non-dimensional compressive in-plane forces ($-\bar{N}_x$) for different antisymmetric angle ply lamination and boundary conditions of stiffened composite hypar shell with cutout

Lamination (Degree)	Boundary conditions					
	Group-I		Group-II		Group-III	
	A CSSC	B CSCS	A FCCF	B FCFC	A FSSF	B FSFS
0	-0.2261 (0.6,0.4)	-0.23069 (0.6,0.4)	-3.8372 (1.0,1.0)	-0.072828 (0.7,0.3)	-10.141 (1.0,1.0)	-0.42598 (1.0,0.9)
(15/-15)	-0.22064 (0.0,0.1)	-0.21061 (0.0,0.1)	-4.5277 (1.0,1.0)	-0.40016 (0.0,0.0)*	-9.5148 (1.0,1.0)	-1.0713 (0.0,0.0)*
(15/-15) ₂	-0.20812 (0.6,0.4)	-0.19707 (0.4,0.6)*	-4.0991 (1.0,1.0)	-0.4439 (0.0,0.0)	-9.4173 (1.0,1.0)	-1.0881 (1.0,1.0)
(15/-15) ₅	-0.21149 (0.6,0.4)	-0.20856 (0.6,0.4)	-3.9392 (1.0,1.0)	-0.465 (0.0,0.0)	-9.4069 (1.0,1.0)	-1.1021 (0.0,0.0)
(30/-30)	-0.22079 (0.6,0.4)	-0.19052 (0.6,0.4)*	-5.8179 (1.0,1.0)	-1.9587 (0.0,0.0)	-9.5995 (1.0,1.0)	-4.1624 (1.0,1.0)
(30/-30) ₂	-0.22306 (0.6,0.4)	-0.21 (0.4,0.6)	-5.2345 (1.0,1.0)	-1.9095 (0.0,0.0)*	-9.5102 (1.0,1.0)	-4.2146 (1.0,1.0)
(30/30) ₅	-0.22126 (0.6,0.4)	-0.21675 (0.6,0.4)	-5.0736 (1.0,1.0)	-1.9192 (0.0,0.0)	-9.494 (1.0,1.0)	-4.2466 (0.0,0.0)
(45/-45)	-0.32889 (0.4,0.6)	-0.32589 (0.6,0.4)	-6.4547 (1.0,1.0)	-5.2902 (1.0,1.0)	-9.8869 (1.0,1.0)	-9.6311 (1.0,1.0)
(45/-45) ₂	-0.32174 (0.6,0.4)	-0.31976 (0.6,0.4)	-5.9539 (1.0,1.0)	-4.864 (0.0,0.0)	-9.6236 (1.0,1.0)	-9.9462 (0.0,0.0)
(45/-45) ₅	-0.31743 (0.6,0.4)	-0.31743 (0.4,0.6)	-5.8547 (1.0,1.0)	-4.7967 (1.0,1.0)	-9.568 (1.0,1.0)	-10.058 (0.0,0.0)
(60/-60)	-0.54396 (0.6,0.4)	-0.5485 (0.4,0.6)	-7.4091 (0.0,0.0)	-6.9079 (0.0,0.0)	-15.804 (0.0,0.0)	-15.74 (1.0,1.0)
(60/-60) ₂	0.52662 (0.6,0.4)	-0.52605 (0.6,0.4)	-6.4334 (0.0,0.0)	-5.9561 (1.0,1.0)	-16.804 (0.0,0.0)	-16.843 (0.0,0.0)
(60/-60) ₅	-0.51857 (0.6,0.4)	-0.51451 (0.6,0.4)	-6.2067 (0.0,0.0)	-5.733 (1.0,1.0)	-17.2 (0.0,0.0)	-17.207 (0.0,0.0)
(75/-75)	-0.89441 (0.4,0.6)	-0.86053 (0.4,0.6)	-6.08 (1.0,1.0)	-2.5635 (1.0,1.0)	-9.8503 (1.0,1.0)	-4.9592 (0.0,0.0)
(75/-75) ₂	-0.80972 (0.4,0.6)	-0.81438 (0.4,0.6)	-6.047 (1.0,1.0)	-1.9671 (0.0,0.0)	-9.3426 (1.0,1.0)	-4.4089 (1.0,1.0)
(75/-75) ₅	-0.81113 (0.6,0.4)	-0.79251 (0.4,0.6)	-6.1081 (1.0,1.0)	-1.7864 (0.0,0.0)	-9.251 (1.0,1.0)	-4.3592 (0.0,0.0)*
90	-1.2582 (0.1,0.1)	-1.3692 (0.0,1.0)	-6.6239 (1.0,1.0)	-1.2853 (0.35,0.6)	-10.557 (0.95,1.0)	-15.316 (0.0,1.0)

$a/b = 1, a/h = 100, a'/b' = 1, c/a = 0.2; E_{11}/E_{22} = 25, G_{23} = 0.2E_{22}, G_{13} = G_{12} = 0.5E_{22}, \nu_{12} = \nu_{21} = 0.25.$

Values in the parenthesis indicates the location (\bar{x}, \bar{y}) of maximum compressive in-plane force in each case.

Asterisk denotes the lowest values of shell actions in each group.

Table 6: Values of maximum non-dimensional tensile in-plane forces ($+\bar{N}_y$) for different antisymmetric angle ply lamination and boundary conditions of stiffened composite hypar shell with cutout

Lamination (Degree)	Boundary conditions					
	Group-I		Group-II		Group-III	
	A CSSC	B CSCS	A FCCF	B FCFC	A FSSF	B FSFS
0	1.5703 (0.1,1.0)	0.95337 (0.6,0.6)	8.1249 (0.0,1.0)	7.3326 (0.0,1.0)	13.253 (0.0,1.0)	13.691 (0.0,1.0)
(15/-15)	1.1795 (0.1,1.0)	0.86069 (0.6,0.6)	12.029 (0.0,1.0)	6.584 (0.0,1.0)	14.505 (0.0,1.0)	12.948 (0.0,1.0)
(15/-15) ₂	1.1585 (0.1,1.0)	0.85032 (0.6,0.6)	10.773 (0.0,1.0)	6.4789 (1.0,0.0)	13.737 (0.0,1.0)	12.842 (1.0,0.0)
(15/-15) ₅	1.1602 (0.1,1.0)	0.85727 (0.6,0.6)	10.591 (0.0,1.0)	6.5179 (0.0,1.0)	13.687 (0.0,1.0)	12.889 (0.0,1.0)
(30/-30)	0.67986 (1.0,0.0)	0.54083 (0.6,0.6)	12.012 (0.0,1.0)	6.2147 (0.0,1.0)	12.702 (0.0,1.0)	11.539 (0.0,1.0)
(30/-30) ₂	0.6406 (0.1,1.0)	0.53009 (0.6,0.6)	11.46 (0.0,1.0)	5.8546 (0.0,1.0)	12.517 (0.0,1.0)	11.569 (0.0,1.0)
(30/30) ₅	0.63949 (0.1,1.0)	0.53243 (0.6,0.6)	11.355 (0.0,1.0)	5.829 (0.0,1.0)	12.524 (0.0,1.0)	11.611 (0.0,1.0)
(45/-45)	0.42775 (1.0,0.0)	0.33923 (0.4,0.4)	9.7855 (0.0,1.0)	5.6655 (0.0,1.0)	10.113 (0.0,1.0)	10.007 (1.0,0.0)
(45/-45) ₂	0.35756 (0.1,1.0)	0.32619 (0.6,0.6)	9.6464 (0.0,1.0)	5.1692 (0.0,1.0)	10.174 (0.0,1.0)	10.123 (1.0,0.0)
(45/-45) ₅	0.36093 (0.4,0.4)	0.32003 (0.6,0.6)	9.6076 (0.0,1.0)	5.0771 (0.0,1.0)	10.206 (0.0,1.0)	10.161 (0.0,1.0)
(60/-60)	0.25317 (0.1,1.0)	0.19181 (0.6,0.6)*	8.3981 (0.0,1.0)	4.209 (0.0,1.0)	9.0008 (0.0,1.0)*	9.2695 (0.0,1.0)
(60/-60) ₂	0.23936 (0.1,1.0)	0.20644 (0.6,0.6)	8.2328 (0.0,1.0)	3.7103 (0.0,1.0)	9.0538 (0.0,1.0)	9.4215 (0.0,1.0)
(60/-60) ₅	0.23216 (0.1,1.0)	0.20562 (0.6,0.6)	8.1888 (0.0,1.0)	3.5806 (0.0,1.0)*	9.0846 (0.0,1.0)	9.4549 (0.0,1.0)
(75/-75)	0.31007 (0.1,1.0)	0.12527 (1.0,1.0)*	7.9453 (0.0,1.0)	3.5359 (1.0,0.0)	9.2688 (0.0,1.0)	9.2695 (1.0,0.0)
(75/-75) ₂	0.25629 (0.1,1.0)	0.16415 (0.4,0.4)	7.7264 (0.0,1.0)	3.1525 (0.0,1.0)	9.2364 (0.0,1.0)	9.2189 (1.0,0.0)
(75/-75) ₅	0.23235 (0.1,1.0)	0.1725 (0.6,0.6)	7.6494 (0.0,1.0)	3.0164 (0.0,1.0)*	9.246 (0.0,1.0)	9.2097 (1.0,0.0)*
90	0.37905 (0.2,1.0)	0.14552 (0.4,0.4)	7.5796 (0.0,1.0)	3.5102 (0.0,1.0)	9.6659 (0.0,1.0)	9.755 (0.0,1.0)

$a/b = 1$, $a/h = 100$, $a'/b' = 1$, $c/a = 0.2$; $E_{11}/E_{22} = 25$, $G_{23} = 0.2E_{22}$, $G_{13} = G_{12} = 0.5E_{22}$, $\nu_{12} = \nu_{21} = 0.25$.

Values in the parenthesis indicates the location (\bar{x}, \bar{y}) of maximum tensile in-plane forces in each case.

Asterisk denotes the lowest values of shell actions in each group.

Table 7: Values of maximum non-dimensional compressive in-plane forces ($-\bar{N}_y$) for different antisymmetric angle ply lamination and boundary conditions of stiffened composite hypar shell with cutout

Lamination (Degree)	Boundary conditions					
	Group-I		Group-II		Group-III	
	A CSSC	B CSCS	A FCCF	B FCFC	A FSSF	B FSFS
0	-1.5446 (0.9,1.0)	-0.95336 (0.4,0.6)	-8.2301 (0.0,0.0)	-7.3323 (1.0,1.0)	-11.319 (0.0,0.0)	-13.69 (1.0,1.0)
(15/-15)	-0.96116 (0.4,0.6)	-0.86069 (0.4,0.6)	-6.4601 (0.0,0.0)	-6.584 (0.0,0.0)	-9.8637 (0.0,0.0)	-12.948 (0.0,0.0)
(15/-15) ₂	-0.87044 (0.4,0.6)	-0.85031 (0.4,0.6)	-6.5404 (0.0,0.0)	-6.4788 (0.0,0.0)	-10.486 (1.0,1.0)	-12.842 (1.0,1.0)
(15/-15) ₅	-0.84528 (0.4,0.6)	-0.85727 (0.4,0.6)	-6.6268 (0.0,0.0)	-6.5177 (0.0,0.0)	-10.958 (1.0,1.0)	-12.889 (0.0,0.0)
(30/-30)	-0.59335 (0.6,0.4)	-0.54083 (0.4,0.6)	-7.6952 (1.0,1.0)	-6.2147 (0.0,0.0)	-12.178 (1.0,1.0)	-11.539 (1.0,1.0)
(30/-30) ₂	-0.57468 (0.6,0.4)	-0.5301 (0.4,0.6)	-6.8396 (1.0,1.0)	-5.8546 (0.0,0.0)	-12.911 (1.0,1.0)	-11.569 (1.0,1.0)
(30/30) ₅	-0.56497 (0.6,0.4)	-0.53242 (0.6,0.4)	-6.645 (1.0,1.0)	-5.8288 (0.0,0.0)	-13.187 (1.0,1.0)	-11.611 (0.0,0.0)
(45/-45)	-0.33559 (0.4,0.4)	-0.33922 (0.6,0.4)	-5.8249 (0.0,0.0)	-5.666 (1.0,1.0)	-9.7042 (0.0,0.0)	-10.007 (1.0,1.0)
(45/-45) ₂	-0.29996 (0.6,0.4)	-0.32619 (0.6,0.4)	-5.3301 (0.0,0.0)	-5.1693 (0.0,0.0)	-9.569 (0.0,0.0)	-10.124 (1.0,1.0)
(45/-45) ₅	-0.2952 (0.6,0.4)	-0.32003 (0.6,0.4)	-5.2398 (0.0,0.0)	-5.077 (1.0,1.0)	-9.5481 (0.0,0.0)	-10.161 (1.0,1.0)
(60/-60)	-0.19497 (0.6,0.4)	-0.19181 (0.4,0.6)*	-4.5275 (0.0,0.0)	-4.2091 (0.0,0.0)	-9.4933 (0.0,0.0)	-9.2697 (1.0,1.0)*
(60/-60) ₂	-0.19597 (0.6,0.4)	-0.20644 (0.6,0.4)	-4.0089 (0.0,0.0)	-3.7104 (1.0,1.0)	-9.4722 (0.0,0.0)	-9.4217 (0.0,0.0)
(60/-60) ₅	-0.19452 (0.6,0.4)	-0.20562 (0.6,0.4)	-3.8755 (0.0,0.0)	-3.5807 (1.0,1.0)	-9.4768 (0.0,0.0)	-9.4551 (0.0,0.0)
(75/-75)	-0.17365 (0.6,0.4)	-0.12527 (0.0,1.0)*	-4.0322 (0.0,0.1)	-3.5358 (0.0,0.0)	-9.4773 (0.0,0.0)	-9.2261 (0.0,0.0)
(75/-75) ₂	-0.19411 (0.6,0.4)	-0.16416 (0.4,0.6)	-3.6081 (0.0,0.1)	-3.1525 (0.0,0.0)	-9.3544 (0.0,0.0)	-9.219 (0.0,0.0)
(75/-75) ₅	-0.19833 (0.6,0.4)	-0.1725 (0.6,0.4)	-3.4788 (0.0,0.1)*	-3.0163 (0.0,0.0)*	-9.3489 (0.0,0.0)	-9.2095 (0.0,0.0)*
90	-0.23827 (0.9,1.0)	-0.14552 (0.6,0.4)	-3.8587 (0.0,0.1)	-3.5101 (0.0,0.0)	-10.191 (0.0,0.0)	-9.7547 (1.0,1.0)

$a/b = 1, a/h = 100, a'/b' = 1, c/a = 0.2; E_{11}/E_{22} = 25, G_{23} = 0.2E_{22}, G_{13} = G_{12} = 0.5E_{22}, \nu_{12} = \nu_{21} = 0.25.$

Values in the parenthesis indicates the location (\bar{x}, \bar{y}) of compressive in-plane forces in each case.

Asterisk denotes the lowest values of shell actions in each group.

Table 8: Values of maximum non-dimensional anticlockwise in-plane shear ($+\bar{N}_{xy}$) for different antisymmetric angle ply lamination and boundary conditions of stiffened composite hypar shell with cutout

Lamination (Degree)	Boundary conditions					
	Group-I		Group-II		Group-III	
	A CSSC	B CSCS	A FCCF	B FCFC	A FSSF	B FSFS
0	0.0 (0.55,0.5)	0.0 (0.55,0.5)	1.0677 (0.1,1.0)	0.029345 (0.6,0.5)	1.475 (0.1,1.0)	0.27826 (0.9,0.0)
(15/-15)	0.0 (0.55,0.5)	0.0 (0.55,0.5)	1.6629 (0.1,1.0)	0.017635 (1.0,0.6)*	1.9098 (0.1,1.0)	0.80412 (0.1,0.0)*
(15/-15) ₂	0.0 (0.55,0.5)	0.0 (0.55,0.5)	1.6889 (0.1,1.0)	0.0024528 (0.4,0.5)*	1.992 (0.1,1.0)	0.83862 (0.1,1.0)
(15/-15) ₅	0.0 (0.55,0.5)	0.0 (0.55,0.5)	1.6906 (0.1,1.0)	0.0033569 (0.4,0.5)	2.0144 (0.1,1.0)	0.84946 (0.9,1.0)
(30/-30)	0.060161 (0.5,0.4)	0.049696 (0.5,0.6)	1.9643 (0.1,1.0)	0.21224 (0.9,0.0)	2.0711 (0.1,1.0)	1.8101 (0.1,1.0)
(30/-30) ₂	0.050709 (0.5,0.4)	0.039623 (0.5,0.6)	1.9164 (0.1,1.0)	0.20183 (0.1,1.0)	2.0612 (0.1,1.0)	1.7764 (0.1,1.0)
(30/30) ₅	0.048996 (0.5,0.4)	0.039251 (0.5,0.4)	1.9068 (0.1,1.0)	0.19954 (0.0,0.9)	2.0664 (0.1,1.0)	1.7653 (0.9,1.0)
(45/-45)	0.10117 (0.6,0.5)	0.10363 (0.5,0.4)	1.7593 (0.0,0.9)	0.94609 (0.9,1.0)	2.2236 (0.1,0.0)	2.2231 (0.1,0.0)
(45/-45) ₂	0.10061 (0.5,0.4)	0.099911 (0.5,0.6)	1.7125 (0.0,0.9)	0.75105 (0.1,0.0)	2.034 (0.1,0.0)	2.084 (0.9,1.0)
(45/-45) ₅	0.10046 (0.5,0.4)	0.098204 (0.5,0.6)	1.7037 (0.0,0.9)	0.71566 (0.0,0.9)	1.9895 (0.1,0.0)	2.0507 (0.9,1.0)
(60/-60)	0.049745 (0.6,0.5)	0.048825 (0.4,0.5)	1.9348 (0.0,0.9)	0.73477 (0.0,0.1)	2.1034 (0.0,0.9)	1.7332 (1.0,0.9)
(60/-60) ₂	0.039239 (0.6,0.5)	0.038134 (0.6,0.5)	1.8923 (0.0,0.9)	0.68062 (1.0,0.9)	2.1083 (0.0,0.9)	1.675 (0.0,0.9)
(60/-60) ₅	0.037443 (0.6,0.5)	0.034525 (0.6,0.5)	1.8787 (0.0,0.9)	0.66164 (1.0,0.9)	2.1132 (0.0,0.9)	1.6642 (1.0,0.9)*
(75/-75)	0.0 (0.55,0.5)	0.0 (0.55,0.5)	1.481 (0.0,0.9)	0.11281 (1.0,0.05)	1.8358 (0.0,0.9)	1.7139 (1.0,0.1)
(75/-75) ₂	0.0038622 (0.0,1.0)*	0.0 (0.55,0.5)	1.5593 (0.0,0.9)	0.081054 (1.0,0.05)	1.9639 (0.0,0.9)	1.7014 (0.0,0.1)
(75/-75) ₅	0.007586 (0.0,1.0)	0.0 (0.55,0.5)*	1.5639 (0.0,0.9)	0.076102 (1.0,0.05)	1.9895 (0.0,0.9)	1.704 (1.0,0.1)
90	0.012027 (0.0,1.0)	0.0 (0.55,0.5)	1.23 (0.1,1.0)	0.12905 (0.0,0.9)	1.5105 (0.0,0.9)	1.2476 (0.0,0.9)

$a/b = 1$, $a/h = 100$, $a'/b' = 1$, $c/a = 0.2$; $E_{11}/E_{22} = 25$, $G_{23} = 0.2E_{22}$, $G_{13} = G_{12} = 0.5E_{22}$, $\nu_{12} = \nu_{21} = 0.25$.

Values in the parenthesis indicates the location (\bar{x}, \bar{y}) of maximum anticlockwise in-plane shear in each case.

Asterisk denotes the lowest values of shell actions in each group.

Table 9: Values of maximum non-dimensional clockwise in-plane shear ($-\bar{N}_{xy}$) for different antisymmetric angle ply lamination and boundary conditions of stiffened composite hypar shell with cutout

Lamination (Degree)	Boundary conditions					
	Group-I		Group-II		Group-III	
	A CSSC	B CSCS	A FCCF	B FCFC	A FSSF	B FSFS
0	-0.81606 (0.7,0.5)	-0.72411 (0.7,0.5)	-6.4021 (0.0,1.0)	-0.75421 (0.9,0.5)	-8.7467 (0.0,1.0)	-3.1941 (1.0,0.0)
(15/-15)	-0.91201 (0.7,0.5)	-0.82463 (0.7,0.5)*	-8.4393 (0.0,1.0)	-0.8656 (0.2,0.5)	-9.6042 (0.0,1.0)	-4.329 (0.0,0.0)*
(15/-15) ₂	-0.93954 (0.7,0.5)	-0.86683 (0.3,0.5)	-8.4212 (0.0,1.0)	-0.83944 (0.2,0.5)	-9.8791 (0.0,1.0)	-4.3948 (1.0,0.0)
(15/-15) ₅	-0.94796 (0.7,0.5)	-0.88329 (0.3,0.5)	-8.3941 (0.0,1.0)	-0.82952 (0.8,0.5)*	-9.9615 (0.0,1.0)	-4.4361 (0.0,1.0)
(30/-30)	-0.96259 (0.7,0.5)	-0.94028 (0.7,0.5)	-9.7512 (0.0,1.0)	-2.0594 (0.0,0.0)	-10.144 (0.0,1.0)	-6.3284 (1.0,1.0)*
(30/-30) ₂	-0.98367 (0.7,0.5)	-0.95642 (0.3,0.5)	-9.6088 (0.0,1.0)	-2.081 (0.0,0.0)	-10.245 (0.0,1.0)	-6.3365 (1.0,1.0)
(30/30) ₅	-0.98776 (0.7,0.5)	-0.96097 (0.7,0.5)	-9.5631 (0.0,1.0)	-2.0998 (0.0,1.0)	-10.286 (0.0,1.0)	-6.3508 (0.0,1.0)
(45/-45)	-0.92099 (0.4,0.6)	-0.91662 (0.4,0.4)	-9.8578 (0.0,1.0)	-4.1137 (1.0,1.0)	-10.134 (0.0,1.0)	-8.3716 (1.0,1.0)
(45/-45) ₂	-0.91888 (0.4,0.4)	-0.90318 (0.7,0.5)	-9.743 (0.0,1.0)	-3.8612 (1.0,1.0)	-10.209 (0.0,1.0)	-8.3429 (1.0,1.0)
(45/-45) ₅	-0.92326 (0.4,0.4)	-0.89661 (0.7,0.5)	-9.7044 (0.0,1.0)	-3.8051 (0.0,1.0)	-10.247 (0.0,1.0)	-8.3367 (0.0,1.0)
(60/-60)	-0.93505 (0.5,0.3)	-0.95646 (0.5,0.7)	-9.2283 (0.0,1.0)	-3.1476 (0.0,0.0)	-9.9836 (0.0,1.0)	-9.0771 (1.0,1.0)
(60/-60) ₂	-0.95 (0.5,0.3)	-0.9614 (0.5,0.7)	-9.0971 (0.0,1.0)	-2.853 (1.0,1.0)	-10.121 (0.0,1.0)	-9.0538 (0.0,0.0)
(60/-60) ₅	-0.95295 (0.5,0.3)	-0.95819 (0.5,0.3)	-9.0465 (0.0,1.0)	-2.7523 (1.0,1.0)	-10.166 (0.0,1.0)	-9.0516 (0.0,0.0)
(75/-75)	-0.88576 (0.5,0.3)	-0.90129 (0.5,0.7)	-7.5545 (0.0,1.0)	-1.0161 (0.5,0.0)	-9.3392 (0.0,1.0)	-8.1809 (1.0,0.0)
(75/-75) ₂	-0.91152 (0.5,0.3)	-0.90488 (0.5,0.7)	-7.6942 (0.0,1.0)	-1.0141 (0.5,0.7)*	-9.7283 (0.0,1.0)	-8.268 (0.0,0.0)
(75/-75) ₅	-0.91993 (0.5,0.3)	-0.9019 (0.5,0.7)*	-7.684 (0.0,1.0)	-1.0563 (0.5,0.7)	-9.8266 (0.0,1.0)	-8.3072 (1.0,0.0)
90	-0.79284 (0.5,0.3)	-0.70155 (0.5,0.7)	-6.1053 (0.0,1.0)	-0.83783 (0.3,0.45)	-8.8142 (0.0,1.0)	-7.1506 (0.0,1.0)

$a/b = 1$, $a/h = 100$, $a'/b' = 1$, $c/a = 0.2$; $E_{11}/E_{22} = 25$, $G_{23} = 0.2E_{22}$, $G_{13} = G_{12} = 0.5E_{22}$, $\nu_{12} = \nu_{21} = 0.25$.

Values in the parenthesis indicates the location (\bar{x}, \bar{y}) of maximum clockwise in-plane shear in each case.

Asterisk denotes the lowest values of shell actions in each group.

Table 10: Values of maximum non-dimensional hogging moments ($+\overline{M}_x$) $\times 10^2$ for different antisymmetric angle ply lamination and boundary conditions of stiffened composite hypar shell with cutout

Lamination (Degree)	Boundary conditions					
	Group-I		Group-II		Group-III	
	A CSSC	B CSCS	A FCCF	B FCFC	A FSSF	B FSFS
0	0.1733 (0.0,0.2)	0.11113 (1.0,0.7)	0.56473 (1.0,1.0)	0.024122 (0.1,0.2)	0.49104 (0.0,1.0)	0.011692 (0.5,0.2)
(15/-15)	0.070218 (0.0,0.8)	0.009076 (0.5,0.6)*	0.58267 (1.0,1.0)	0.018106 (1.0,0.0)*	0.21799 (0.6,1.0)	0.042386 (0.1,1.0)
(15/-15) ₂	0.073993 (0.0,0.8)	0.020888 (0.0,0.7)	0.47933 (1.0,1.0)	0.054734 (1.0,0.0)	0.17383 (0.0,1.0)	0.014633 (0.9,1.0)
(15/-15) ₅	0.078154 (0.0,0.8)	0.03203 (1.0,0.3)	0.46034 (1.0,1.0)	0.070948 (0.0,1.0)	0.25984 (0.0,1.0)	0.008737 (0.5,0.9)*
(30/-30)	0.035442 (0.5,0.4)	0.033458 (0.5,0.6)	0.43318 (0.1,1.0)	0.078403 (0.1,0.0)*	0.42881 (0.1,1.0)	0.21199 (0.1,0.0)
(30/-30) ₂	0.046301 (0.0,0.8)	0.019482 (0.5,0.4)	0.40742 (1.0,0.9)	0.13146 (0.1,1.0)	0.20589 (0.1,1.0)	0.084094 (0.9,0.0)
(30/30) ₅	0.065945 (0.0,0.8)	0.017297 (1.0,0.8)*	0.40778 (1.0,0.9)	0.18042 (0.0,1.0)	0.16959 (0.1,0.9)	0.022879 (0.0,0.1)*
(45/-45)	0.07068 (0.6,0.5)	0.070597 (0.4,0.5)	0.54376 (0.1,1.0)	0.39356 (0.9,1.0)	0.53034 (0.1,1.0)	0.46518 (0.9,1.0)
(45/-45) ₂	0.059565 (0.0,0.8)	0.040782 (0.4,0.5)	0.4976 (1.0,0.9)	0.48243 (0.1,1.0)	0.30771 (0.1,1.0)	0.18732 (0.1,0.0)
(45/-45) ₅	0.10176 (0.0,0.8)	0.04585 (0.0,0.2)	0.48296 (1.0,0.9)	0.47989 (0.1,1.0)	0.3096 (0.1,0.9)	0.088067 (0.1,0.1)
(60/-60)	0.12571 (0.6,0.5)	0.12601 (0.4,0.5)	0.75082 (0.0,0.9)	0.38716 (0.1,0.0)	0.88609 (0.0,0.1)	0.88041 (0.0,0.9)
(60/-60) ₂	0.093456 (0.0,0.8)	0.068749 (0.6,0.5)	0.76655 (0.1,0.0)	0.66116 (0.1,1.0)	0.37744 (0.0,0.1)	0.40718 (1.0,0.1)
(60/-60) ₅	0.17278 (0.0,0.8)	0.11344 (1.0,0.2)	0.84427 (0.1,0.0)	0.73403 (0.9,1.0)	0.33143 (0.1,0.95)	0.26611 (0.5,0.7)
(75/-75)	0.17833 (0.4,0.5)	0.17252 (0.6,0.5)	0.45453 (0.0,0.9)	0.22302 (1.0,0.0)	1.4684 (0.0,0.1)	1.4223 (1.0,0.9)
(75/-75) ₂	0.31203 (0.0,0.85)	0.17805 (1.0,0.8)	0.55158 (0.1,0.0)	0.49388 (0.0,0.0)	0.69868 (0.0,0.1)	0.68733 (1.0,0.1)
(75/-75) ₅	0.43019 (0.0,0.8)	0.32431 (0.0,0.2)	0.77332 (0.0,1.0)	0.56095 (1.0,0.0)	0.43899 (0.0,1.0)	0.43072 (0.5,0.7)
90	1.2084 (0.0,0.8)	1.1036 (0.0,0.8)	1.6053 (0.0,1.0)	0.83884 (0.5,0.7)	1.5659 (0.0,1.0)	0.63796 (0.5,0.7)

$a/b = 1$, $a/h = 100$, $a'/b' = 1$, $c/a = 0.2$; $E_{11}/E_{22} = 25$, $G_{23} = 0.2E_{22}$, $G_{13} = G_{12} = 0.5E_{22}$, $\nu_{12} = \nu_{21} = 0.25$.

Values in the parenthesis indicates the location (\bar{x}, \bar{y}) of maximum hogging moment in each case.

Asterisk denotes the lowest values of shell actions in each group.

Table 11: Values of maximum non-dimensional sagging moments ($-\bar{M}_x$) $\times 10^2$ for different antisymmetric angle ply lamination and boundary conditions of stiffened composite hypar shell with cutout

Lamination (Degree)	Boundary conditions					
	Group-I		Group-II		Group-III	
	A CSSC	B CSCS	A FCCF	B FCFC	A FSSF	B FSFS
0	-0.07217 (0.1,0.2)	-0.04077 (0.5,0.8)	-0.15652 (0.1,1.0)	-0.01237 (0.5,0.7)	-0.12979 (0.2,1.0)	-0.02785 (0.1,0.1)
(15/-15)	-0.07661 (0.1,0.8)	-0.05455 (0.7,0.2)	-0.19706 (0.5,1.0)	-0.05043 (0.9,0.4)	-0.19147 (0.8,1.0)	-0.23389 (0.0,1.0)
(15/-15) ₂	-0.06434 (0.1,0.8)	-0.03983 (0.3,0.2)	-0.11269 (0.5,1.0)	-0.03299 (0.1,0.4)	-0.1124 (0.2,1.0)	-0.09701 (1.0,1.0)
(15/-15) ₅	-0.05774 (0.1,0.8)	-0.03257 (0.3,0.2)*	-0.09048 (0.5,1.0)	-0.02126 (0.9,0.6)*	-0.09444 (0.2,1.0)	-0.02251 (0.2,0.1)*
(30/-30)	-0.12128 (0.7,0.5)	-0.11661 (0.7,0.5)	-1.1612 (0.0,1.0)	-0.17063 (1.0,0.0)	-1.0995 (0.0,0.0)	-0.87767 (1.0,1.0)
(30/-30) ₂	-0.0806 (0.1,0.8)	-0.0638 (0.3,0.2)	-0.31795 (0.0,1.0)	-0.07998 (0.8,0.6)	-0.34152 (1.0,1.0)	-0.35251 (1.0,0.0)
(30/30) ₅	-0.06168 (0.1,0.8)	-0.04251 (0.7,0.2)*	-0.09197 (0.8,0.9)	-0.05672 (0.95,0.5)*	-0.09418 (0.3,0.9)	-0.06886 (0.8,0.9)*
(45/-45)	-0.21697 (0.4,0.6)	-0.21721 (0.4,0.4)	-2.4813 (0.0,1.0)	-0.83445 (1.0,1.0)	-2.3619 (0.0,1.0)	-2.1447 (1.0,1.0)
(45/-45) ₂	-0.1145 (0.6,0.6)	-0.11326 (0.6,0.6)	-0.89639 (0.0,1.0)	-0.16664 (0.5,0.0)	-0.87451 (0.0,1.0)	-0.83756 (0.0,0.0)
(45/-45) ₅	-0.08484 (0.1,0.9)	-0.0633 (0.3,0.8)	-0.14748 (0.3,0.9)	-0.12532 (0.1,0.8)	-0.16408 (0.3,0.9)	-0.11715 (0.1,0.5)
(60/-60)	-0.34231 (0.5,0.3)	-0.34383 (0.5,0.7)	-3.09 (0.0,1.0)	-1.0957 (1.0,1.0)	-4.1246 (0.0,0.0)	-4.1127 (0.0,1.0)
(60/-60) ₂	-0.1933 (0.2,0.9)	-0.1738 (0.5,0.7)	-0.95147 (0.0,1.0)	-0.23158 (0.5,0.0)	-1.6648 (0.0,0.0)	-1.8092 (1.0,1.0)
(60/-60) ₅	-0.143 (0.2,0.9)	-0.1143 (0.8,0.9)	-0.22949 (0.3,1.0)	-0.15333 (0.1,0.2)	-0.30349 (0.0,0.0)	-0.45751 (0.0,1.0)
(75/-75)	-0.57022 (0.5,0.3)	-0.58318 (0.5,0.3)	-1.88 (0.0,0.9)	-0.68 (1.0,1.0)	-5.33 (0.0,0.0)	-5.20 (0.0,1.0)
(75/-75) ₂	-0.36472 (0.2,0.9)	-0.33128 (0.6,0.7)	-0.67973 (0.2,1.0)	-0.36461 (0.5,0.0)	-2.448 (0.0,0.0)	-2.4407 (0.0,0.0)
(75/-75) ₅	-0.29287 (0.2,0.9)	-0.2382 (0.8,0.9)	-0.63808 (0.2,1.0)	-0.1734 (0.5,1.0)	-0.89725 (0.0,0.0)	-0.91497 (0.0,0.0)
90	-0.5455 (0.8,0.8)	-0.38428 (0.3,0.9)	-1.105 (0.2,1.0)	-0.11682 (0.6,0.5)	-1.1064 (0.3,1.0)	-0.31231 (0.0,1.0)

$a/b = 1, a/h = 100, a'/b' = 1, c/a = 0.2; E_{11}/E_{22} = 25, G_{23} = 0.2E_{22}, G_{13} = G_{12} = 0.5E_{22}, \nu_{12} = \nu_{21} = 0.25.$

Values in the parenthesis indicates the location (\bar{x}, \bar{y}) of maximum sagging moment in each case.

Asterisk denotes the lowest values of shell actions in each group.

Table 12: Values of maximum non-dimensional hogging moments ($+\bar{M}_y$) $\times 10^2$ for different antisymmetric angle ply lamination and boundary conditions of stiffened composite hypar shell with cutout

Lamination (Degree)	Boundary conditions					
	Group-I		Group-II		Group-III	
	A CSSC	B CSCS	A FCCF	B FCFC	A FSSF	B FSFS
0	1.0989 (0.3,1.0)	0.14567 (0.8,0.4)	1.9282 (0.0,1.0)	1.5501 (1.0,1.0)	1.9577 (0.0,1.0)	0.76568 (0.0,1.0)
(15/-15)	0.18294 (0.5,0.6)	0.17602 (0.5,0.6)	0.60494 (0.1,1.0)	0.49154 (1.0,0.0)	1.4971 (0.9,1.0)	0.43213 (0.1,1.0)
(15/-15) ₂	0.33502 (0.1,1.0)	0.094348 (0.5,0.4)	0.59732 (0.0,0.0)	0.81579 (1.0,0.0)	0.71556 (0.9,1.0)	0.13878 (0.9,1.0)*
(15/-15) ₅	0.42442 (0.05,1.0)	0.043018 (0.5,0.6)	0.71295 (0.0,0.0)	0.95353 (0.0,1.0)	0.51698 (0.0,1.0)	0.23817 (1.0,0.2)
(30/-30)	0.13018 (0.5,0.4)	0.12592 (0.5,0.6)	0.65895 (0.1,1.0)	0.29714 (0.1,0.0)*	0.64229 (0.1,1.0)	0.45894 (0.1,0.0)
(30/-30) ₂	0.12439 (0.2,1.0)	0.068785 (0.5,0.4)	0.68264 (1.0,0.9)	0.68264 (0.05,1.0)	0.39622 (0.0,0.9)	0.23195 (1.0,0.9)
(30/30) ₅	0.19502 (0.2,1.0)	0.030276 (0.5,0.4)	0.69153 (1.0,0.9)	0.65549 (0.0,1.0)	0.41284 (0.1,0.9)	0.21265 (0.0,0.1)
(45/-45)	0.070755 (0.5,0.4)	0.0715 (0.5,0.6)	0.63083 (0.0,0.9)	0.54743 (0.9,1.0)	0.62673 (0.0,0.9)	0.48471 (1.0,0.9)
(45/-45) ₂	0.073105 (0.2,1.0)	0.041513 (0.5,0.6)	0.63658 (0.1,0.0)	0.63803 (0.1,1.0)	0.33191 (0.0,0.9)	0.28047 (0.0,0.1)
(45/-45) ₅	0.11192 (0.2,1.0)	0.03273 (0.0,0.2)	0.62425 (0.1,0.0)	0.63063 (0.1,1.0)	0.42522 (0.1,0.9)	0.17798 (0.05,0.1)
(60/-60)	0.0343 (0.6,0.5)	0.034695 (0.4,0.5)	0.52066 (0.1,0.0)	0.45694 (0.1,0.0)	0.39142 (0.0,0.9)	0.35426 (0.0,0.1)
(60/-60) ₂	0.054548 (0.2,1.0)	0.020571 (0.4,0.5)*	0.57856 (0.1,0.0)	0.50927 (0.1,1.0)	0.20942 (0.05,0.9)	0.22069 (1.0,0.9)
(60/-60) ₅	0.071821 (0.2,1.0)	0.032858 (1.0,0.2)	0.58183 (0.1,0.0)	0.51212 (0.9,1.0)	0.24199 (0.1,0.9)	0.17021 (0.1,0.9)
(75/-75)	0.074306 (0.2,1.0)	0.010284 (0.6,0.5)*	0.6692 (0.0,0.0)	0.64125 (1.0,0.0)	0.34954 (0.0,1.0)	0.22477 (1.0,0.4)
(75/-75) ₂	0.077768 (0.2,1.0)	0.014925 (1.0,0.9)	0.53987 (0.0,0.0)	0.48786 (0.0,0.0)	0.3024 (0.0,1.0)	0.12056 (0.0,0.0)*
(75/-75) ₅	0.081093 (0.2,1.0)	0.026659 (1.0,0.9)	0.50161 (0.0,0.0)	0.4395 (1.0,0.0)*	0.29251 (0.0,1.0)	0.1519 (1.0,1.0)
90	0.16104 (0.8,1.0)	0.019233 (0.0,0.9)	0.52068 (0.0,1.0)	0.39293 (0.0,1.0)	0.4542 (0.0,1.0)	0.2274 (0.0,1.0)

$a/b = 1$, $a/h = 100$, $a'/b' = 1$, $c/a = 0.2$; $E_{11}/E_{22} = 25$, $G_{23} = 0.2E_{22}$, $G_{13} = G_{12} = 0.5E_{22}$, $\nu_{12} = \nu_{21} = 0.25$.

Values in the parenthesis indicates the location (\bar{x}, \bar{y}) of maximum hogging moments in each case.

Asterisk denotes the lowest values of shell actions in each group.

Table 13: Values of maximum non-dimensional sagging moment ($-\bar{M}_y$) $\times 10^2$ for different antisymmetric angle ply lamination and boundary conditions of stiffened composite hypar shell with cutout

Lamination (Degree)	Boundary conditions					
	Group-I		Group-II		Group-III	
	A CSSC	B CSCS	A FCCF	B FCFC	A FSSF	B FSFS
0	-0.5569 (0.2,0.2)	-0.4939 (0.3,0.2)	-1.0872 (0.0,0.8)	-0.53002 (0.0,0.5)	-1.0741 (0.0,0.7)	-0.48039 (1.0,0.5)
(15/-15)	-0.5711 (0.7,0.5)	-0.51574 (0.7,0.5)	-2.5698 (0.0,1.0)	-0.70504 (0.2,0.7)	-6.0338 (1.0,1.0)	-2.274 (0.0,1.0)
(15/-15) ₂	-0.36225 (0.2,0.2)	-0.33883 (0.3,0.2)	-0.55374 (0.0,0.75)	-0.46423 (0.8,0.4)	-2.797 (1.0,1.0)	-0.86614 (1.0,1.0)
(15/-15) ₅	-0.27309 (0.2,0.2)	-0.24825 (0.3,0.2)	-0.58115 (0.0,0.75)	-0.31348 (1.0,0.7)	-0.96784 (1.0,1.0)	-0.30621 (0.0,0.5)
(30/-30)	-0.34589 (0.7,0.5)	-0.33118 (0.7,0.5)	-2.7859 (0.0,1.0)	-0.44972 (0.8,0.6)	-3.1552 (1.0,1.0)	-1.9656 (1.0,0.0)
(30/-30) ₂	-0.19022 (0.2,0.8)	-0.18219 (0.7,0.8)	-0.86671 (0.0,1.0)	-0.26521 (0.8,0.6)	-1.2467 (1.0,1.0)	-0.74163 (1.0,0.0)
(30/30) ₅	-0.14064 (0.1,0.8)	-0.11837 (0.7,0.2)	-0.21554 (0.0,0.7)	-0.1902 (0.0,0.5)	-0.2256 (0.05,0.7)	-0.19999 (0.0,0.5)
(45/-45)	-0.21819 (0.4,0.6)	-0.21759 (0.4,0.4)	-1.7462 (0.0,1.0)	-.2829 (0.5,0.0)	-1.6292 (0.0,1.0)	-1.4003 (1.0,1.0)
(45/-45) ₂	-0.11564 (0.1,0.9)	-0.11318 (0.6,0.6)	-0.5536 (0.0,1.0)	-0.20584 (0.5,1.0)	-0.5317 (0.0,1.0)	-0.4722 (0.0,0.0)
(45/-45) ₅	-0.09188 (0.1,0.9)	-0.06634 (0.2,0.1)	-0.1338 (0.1,0.7)	-0.14615 (0.5,0.0)	-0.16154 (0.3,0.1)	-.13433 (0.05,0.5)
(60/-60)	-0.12133 (0.5,0.3)	-0.12091 (0.5,0.7)	-0.4647 (0.0,1.0)	-0.16361 (0.0,0.5)	-0.58686 (0.0,0.0)	-0.64936 (0.0,1.0)
(60/-60) ₂	-0.083579 (0.2,0.9)	-0.070521 (0.8,0.1)	-0.097655 (0.1,0.2)	-0.10789 (0.5,0.0)	-0.12226 (0.0,0.0)	-0.10789 (1.0,0.0)
(60/-60) ₅	-0.066557 (0.2,0.9)	-0.049949 (0.8,0.9)*	-0.086694 (0.0,0.3)*	-0.089522 (1.0,0.3)	-0.080367 (0.05,0.7)*	-0.096107 (0.95,0.3)
(75/-75)	-0.07812 (0.2,0.9)	-0.06465 (0.8,0.9)	-0.19869 (0.0,0.5)	-.20524 (1.0,0.5)	-0.19122 (0.0,0.5)	-0.20417 (0.0,0.5)
(75/-75) ₂	-0.06825 (0.2,0.9)	-0.05064 (0.8,0.9)	-0.11075 (0.0,0.5)	-0.12232 (0.0,0.5)	-0.10259 (0.0,0.5)	-0.12641 (0.0,0.3)
(75/-75) ₅	-0.0627 (0.2,0.9)	-0.04301 (0.8,0.9)*	-0.08809 (0.0,0.5)*	-0.10272 (0.0,0.3)	-0.08626 (0.0,0.3)*	-0.11185 (1.0,0.3)
90	-0.071805 (0.2,0.9)	-0.048512 (0.2,0.9)	-0.145 (0.0,0.9)	-0.13011 (1.0,0.7)	-0.13213 (0.0,0.8)	-0.13244 (1.0,0.7)

$a/b = 1, a/h = 100, a'/b' = 1, c/a = 0.2; E_{11}/E_{22} = 25, G_{23} = 0.2E_{22}, G_{13} = G_{12} = 0.5E_{22}, \nu_{12} = \nu_{21} = 0.25.$

Values in the parenthesis indicates the location (\bar{x}, \bar{y}) of maximum sagging moment in each case.

Asterisk denotes the lowest values of shell actions in each group.

Table 14: Values of maximum non-dimensional anticlockwise twisting moments ($+\bar{M}_{xy}$) $\times 10^2$ for different antisymmetric angle ply lamination and boundary conditions of stiffened composite hypar shell with cutout

Lamination (Degree)	Boundary conditions					
	Group-I		Group-II		Group-III	
	A CSSC	B CSCS	A FCCF	B FCFC	A FSSF	B FSFS
0	0.037944 (0.1,0.0)	0.031328 (0.9,1.0)	0.12088 (0.1,1.0)	0.024386 (0.0,0.3)	0.11372 (0.0,0.0)	0.090819 (0.0,0.0)
(15/-15)	0.088735 (0.6,0.6)	0.080738 (0.4,0.4)	0.923 (0.0,1.0)	0.43923 (0.0,1.0)	1.0578 (0.0,1.0)	0.82629 (0.0,1.0)
(15/-15) ₂	0.057772 (0.4,0.4)	0.052299 (0.4,0.4)	0.35989 (0.1,0.9)	0.24023 (1.0,0.0)	0.37682 (0.1,0.9)	0.35256 (1.0,0.0)
(15/-15) ₅	0.040785 (1.0,0.9)*	0.031211 (0.4,0.4)*	0.32007 (0.1,0.9)	0.11952 (0.0,1.0)*	0.32814 (0.1,0.9)	0.13407 (1.0,0.1)*
(30/-30)	0.18995 (1.0,0.0)	0.10485 (0.6,0.6)	1.9754 (0.0,1.0)	0.91723 (0.0,1.0)	1.9759 (0.0,1.0)	1.5173 (0.0,1.0)
(30/-30) ₂	0.07692 (0.4,0.4)	0.068537 (0.6,0.6)	0.70675 (0.0,1.0)	0.48562 (0.0,1.0)	0.7438 (0,1,0.9)	0.65793 (1.0,0.0)
(30/30) ₅	0.045777 (0.4,0.4)	0.040937 (0.4,0.4)	0.58772 (0.1,0.9)	0.2484 (0.05,0.9)	0.60932 (0.1,0.9)	0.25235 (1.0,0.1)
(45/-45)	0.21947 (1.0,0.0)	0.11146 (0.4,0.4)	2.1835 (0.0,1.0)	1.3376 (1.0,0.0)	2.1452 (0.0,1.0)	1.9668 (1.0,0.0)
(45/-45) ₂	0.075312 (0.4,0.4)	0.073197 (0.4,0.4)	0.84521 (0.1,0.9)	0.68613 (0.0,1.0)	0.89207 (0.1,0.9)	0.83756 (0.0,1.0)
(45/-45) ₅	0.045154 (0.4,0.4)	0.043868 (0.6,0.6)	0.68098 (0.1,0.9)	0.43169 (0.1,0.9)	0.707 (0.1,0.9)	0.43052 (0.1,0.9)
(60/-60)	0.11493 (1.0,0.0)	0.1039 (0.4,0.4)	1.5035 (0.0,1.0)	1.0423 (0.0,1.0)	1.5841 (0.0,1.0)	1.6624 (0.0,1.0)
(60/-60) ₂	0.072134 (0.6,0.6)	0.067079 (0.4,0.4)	0.68201 (0.1,0.9)	0.61209 (0.0,1.0)	0.72278 (0.1,0.9)	0.73891 (1.0,0.0)
(60/-60) ₅	0.042195 (0.,6,0.6)	0.042783 (0.9,1.0)	0.60475 (0.1,0.9)	0.39865 (0.1,0.9)	0.62474 (0.1,0.9)	0.48929 (0.9,0.1)
(75/-75)	0.08634 (0.4,0.4)	0.084457 (0.9,1.0)	0.42859 (1.0,0.05)	0.35338 (1.0,0.0)	0.54137 (0.05,1.0)	0.29934 (0.95,0.1)
(75/-75) ₂	0.060973 (0.2,0.0)	0.068926 (0.9,1.0)	0.33476 (0.1,0.9)	0.29418 (0.0,1.0)	0.35635 (0.1,0.9)	0.2705 (0.9,0.1)
(75/-75) ₅	0.05751 (0.9,0.9)	0.061555 (0.9,1.0)	0.31778 (0.1,0.9)	0.24969 (1.0,0.0)*	0.33055 (0.1,0.9)	0.23722 (0.9,0.1)*
90	0.094868 (0.0,0.85)	0.094647 (0.0,0.9)	0.098128 (0.1,1.0)	0.074555 (0.2,0.9)	0.12883 (0.0,0.0)	0.095647 (0.0,0.0)

$a/b = 1$, $a/h = 100$, $a'/b' = 1$, $c/a = 0.2$; $E_{11}/E_{22} = 25$, $G_{23} = 0.2E_{22}$, $G_{13} = G_{12} = 0.5E_{22}$, $\nu_{12} = \nu_{21} = 0.25$.
 Values in the parenthesis indicates the location (\bar{x}, \bar{y}) of maximum anticlockwise twisting moment in each case.
 Asterisk denotes the lowest values of shell actions in each group.

Table 15: Values of maximum non-dimensional clockwise twisting moments ($-\bar{M}_{xy}$) $\times 10^2$ for different antisymmetric angle ply lamination and boundary conditions of stiffened composite hypar shell with cutout

Lamination (Degree)	Boundary conditions					
	Group-I		Group-II		Group-III	
	A CSSC	B CSCS	A FCCF	B FCFC	A FSSF	B FSFS
0	-0.055845 (1.0,0.0)	-0.031327 (0.9,0.0)	-0.24013 (0.0,1.0)	-0.024384 (0.0,0.7)	-0.23557 (0.0,1.0)	-0.090831 (0.0,1.0)
(15/-15)	-0.082597 (0.4,0.6)	-0.080739 (0.4,0.6)	-0.46078 (1.0,1.0)	-0.43923 (0.0,0.0)	-0.65365 (1.0,1.0)	-0.82627 (0.0,0.0)
(15/-15) ₂	-0.054896 (0.6,0.4)	-0.052298 (0.4,0.6)	-0.24402 (1.0,1.0)	-0.24022 (0.0,0.0)	-0.32104 (0.9,0.9)	-0.35257 (1.0,1.0)
(15/-15) ₅	-0.045312 (1.0,0.1)	-0.031211 (0.6,0.4)*	-0.20873 (0.9,0.9)*	-0.11952 (0.0,0.0)*	-0.25284 (0.9,0.9)	-0.13408 (1.0,0.9)*
(30/-30)	-0.11314 (0.6,0.4)	-0.10485 (0.6,0.4)	-1.3121 (1.0,1.0)	-0.91722 (0.0,0.0)	-1.7703 (1.0,1.0)	-1.5173 (0.0,0.0)
(30/-30) ₂	-0.072684 (0.6,0.4)	-0.068538 (0.6,0.4)	-0.59443 (1.0,1.0)	-0.48561 (0.0,0.0)	-0.70074 (1.0,1.0)	-0.65792 (1.0,1.0)
(30/30) ₅	-0.043701 (0.4,0.6)	-0.040939 (0.6,0.4)*	-0.42815 (0.9,0.9)	-0.24837 (0.05,0.1)	-0.48183 (0.9,0.9)	-0.25232 (1.0,0.9)
(45/-45)	-0.11261 (0.4,0.6)	-0.11146 (0.6,0.4)	-1.3708 (0.0,0.0)	-1.3377 (1.0,1.0)	-1.8555 (0.0,0.0)	-1.9668 (1.0,1.0)
(45/-45) ₂	-0.07387 (0.4,0.6)	-0.0732 (0.4,0.6)	-0.70037 (0.0,0.0)	-0.68614 (0.0,0.0)	-0.71911 (0.0,0.0)	-0.8376 (0.0,0.0)
(45/-45) ₅	-0.05117 (0.1,0.9)	-0.04387 (0.4,0.6)	-0.41485 (0.1,0.1)	-0.43166 (0.1,0.1)	-0.43291 (0.05,0.1)	-0.43053 (0.9,0.9)
(60/-60)	-0.10681 (0.6,0.4)	-0.1039 (0.4,0.6)	-1.0968 (0.0,0.0)	-1.0423 (0.0,0.0)	-1.6311 (0.0,0.0)	-1.6624 (0.0,0.0)
(60/-60) ₂	-0.069411 (0.6,0.4)	-0.067078 (0.6,0.4)	-0.64052 (0.0,0.0)	-0.61206 (0.0,0.0)	-0.68785 (0.0,0.0)	-0.7389 (1.0,1.0)
(60/-60) ₅	-0.049518 (0.1,0.9)	-0.042783 (0.9,0.0)	-0.4098 (0.0,0.0)	-0.3987 (0.9,0.9)	-0.50166 (0.1,0.1)	-0.4893 (0.9,0.9)
(75/-75)	-0.08036 (0.4,0.6)	-0.08445 (0.1,1.0)	-0.38089 (1.0,1.0)	-0.35338 (1.0,1.0)	-0.39001 (0.95,1.0)	-0.29929 (0.05,1.0)
(75/-75) ₂	-0.06047 (0.9,0.0)	-0.06892 (0.9,0.0)	-0.30561 (0.0,0.0)	-0.29418 (0.0,0.0)	-0.27639 (0.05,0.1)	-0.2705 (0.1,0.1)
(75/-75) ₅	-0.05426 (0.9,0.0)	-0.06155 (0.1,1.0)	-0.26932 (0.0,0.0)	-0.24967 (0.0,0.0)	-0.24089 (0.1,0.1)	-0.23721 (0.9,0.8)*
90	-0.084457 (0.0,0.1)	-0.094646 (0.0,0.1)	-0.18059 (1.0,1.0)	-0.074542 (0.2,0.1)	-0.10505 (0.0,1.0)	-0.095682 (0.0,1.0)

$a/b = 1, a/h = 100, a'/b' = 1, c/a = 0.2; E_{11}/E_{22} = 25, G_{23} = 0.2E_{22}, G_{13} = G_{12} = 0.5E_{22}, \nu_{12} = \nu_{21} = 0.25.$

Values in the parenthesis indicates the location (\bar{x}, \bar{y}) of maximum clockwise twisting moment in each case.

Asterisk denotes the lowest values of shell actions in each group.

Table 16: Shell options arranged according to ascending order of positive values of shell actions different antisymmetric angle ply lamination and boundary conditions of stiffened composite hypar shell with cutout

Non-dimensional Shell Action	Non-dimensional coordinates (\bar{x} , \bar{y})	Shell actions at each layer
\bar{N}_x	$\bar{x} = 0.6, \bar{y} = 0.6$	CSCS/(30/-30)
	$\bar{x} = 0.6, \bar{y} = 0.6$	CSCS/ (15/-15) ₂
	$\bar{x} = 0.0, \bar{y} = 1.0$	FCFC/ (15/-15)
	$\bar{x} = 0.0, \bar{y} = 1.0$	FCFC/(75/-75) ₅
	$\bar{x} = 0.0, \bar{y} = 1.0$	FSFS/ (15/-15)
\bar{N}_y	$\bar{x} = 0.0, \bar{y} = 1.0$	FSFS/ (30/-30)
	$\bar{x} = 1.0, \bar{y} = 1.0$	CSCS/ (75/-75)
	$\bar{x} = 0.6, \bar{y} = 0.6$	CSCS/ (60/-60)
	$\bar{x} = 0.0, \bar{y} = 1.0$	FCFC/(75/-75) ₅
	$\bar{x} = 0.0, \bar{y} = 1.0$	FCFC/(60/-60) ₅
\bar{N}_{xy}	$\bar{x} = 0.0, \bar{y} = 1.0$	FSSF/(60/-60)
	$\bar{x} = 1.0, \bar{y} = 0.0$	FSFS/(75/-75) ₅
	$\bar{x} = 0.55, \bar{y} = 0.5$	CSCS/(75/-75) ₅
	$\bar{x} = 0.0, \bar{y} = 1.0$	CSSC/(75/-75) ₂
	$\bar{x} = 0.4, \bar{y} = 0.5$	FCFC/(15/-15) ₂
\bar{M}_x	$\bar{x} = 1.0, \bar{y} = 0.6$	FCFC/ (15/-15)
	$\bar{x} = 0.1, \bar{y} = 0.0$	FSFS/ (15/-15)
	$\bar{x} = 1.0, \bar{y} = 0.9$	FSFS/(60/-60) ₅
	$\bar{x} = 0.5, \bar{y} = 0.6$	CSCS/(15/-15)
	$\bar{x} = 1.0, \bar{y} = 0.8$	CSCS/(30/-30) ₅
\bar{M}_y	$\bar{x} = 1.0, \bar{y} = 0.0$	FCFC/(15/-15)
	$\bar{x} = 0.1, \bar{y} = 0.0$	FCFC/(30/-30)
	$\bar{x} = 0.5, \bar{y} = 0.9$	FSFS/(15/-15) ₅
	$\bar{x} = 0.0, \bar{y} = 0.1$	FSFS/(30/-30) ₅
	$\bar{x} = 0.6, \bar{y} = 0.5$	CSCS/(75/-75)
\bar{M}_{xy}	$\bar{x} = 0.4, \bar{y} = 0.5$	CSCS/ (60/-60) ₂
	$\bar{x} = 0.1, \bar{y} = 0.0$	FCFC/(30/-30)
	$\bar{x} = 1.0, \bar{y} = 0.0$	FCFC/(75/-75) ₅
	$\bar{x} = 0.0, \bar{y} = 0.0$	FSFS/(75/-75) ₂
	$\bar{x} = 0.9, \bar{y} = 1.0$	FSFS/ (15/-15) ₂
\bar{M}_{xy}	$\bar{x} = 0.4, \bar{y} = 0.4$	CSCS/(15/-15) ₅
	$\bar{x} = 1.0, \bar{y} = 0.9$	CSSC/ (15/-15) ₅
	$\bar{x} = 0.0, \bar{y} = 1.0$	FCFC/ (15/-15) ₅
	$\bar{x} = 1.0, \bar{y} = 0.0$	FCFC/ (75/-75) ₅
	$\bar{x} = 1.0, \bar{y} = 0.1$	FSFS/ (15/-15) ₅
	$\bar{x} = 0.9, \bar{y} = 0.1$	FSFS/ (75/-75) ₅

Table 17: Shell options arranged according to ascending order of negative values of shell actions of different anti-symmetric angle ply lamination and boundary conditions of stiffened composite hypar shell with cutout

Non-dimensional Shell Action	Non-dimensional coordinates (\bar{x}, \bar{y})	Shell actions at each layer
\bar{w}	$\bar{x} = 0.5, \bar{y} = 0.6$	CSCS/(45/-45) ₅
	$\bar{x} = 0.5, \bar{y} = 0.6$	CSCS/(60/-60) ₅
	$\bar{x} = 0.0, \bar{y} = 0.5$	FCFC/(15/-15)
	$\bar{x} = 0.0, \bar{y} = 0.5$	FCFC/(30/-30) ₂
	$\bar{x} = 1.0, \bar{y} = 0.5$	FSFS/(15/-15) ₅
	$\bar{x} = 1.0, \bar{y} = 0.5$	FSFS/(30/-30) ₅
\bar{N}_x	$\bar{x} = 0.6, \bar{y} = 0.4$	CSCS/(30/-30)
	$\bar{x} = 0.4, \bar{y} = 0.6$	CSCS/(15/-15) ₂
	$\bar{x} = 0.0, \bar{y} = 0.0$	FCFC/(15/-15)
	$\bar{x} = 0.0, \bar{y} = 0.0$	FCFC/(30/-30) ₂
	$\bar{x} = 0.0, \bar{y} = 0.0$	FSFS/(15/-15)
	$\bar{x} = 0.0, \bar{y} = 0.0$	FSFS/(75/-75) ₅
\bar{N}_y	$\bar{x} = 0.0, \bar{y} = 1.0$	CSCS/(75/-75)
	$\bar{x} = 0.4, \bar{y} = 0.6$	CSSC/(60/-60)
	$\bar{x} = 0.0, \bar{y} = 0.0$	FCFC/(75/-75) ₅
	$\bar{x} = 0.0, \bar{y} = 0.1$	FCCF/(75/-75) ₅
	$\bar{x} = 0.0, \bar{y} = 0.0$	FSFS/(75/-75) ₅
	$\bar{x} = 1.0, \bar{y} = 1.0$	FSSF/(60/-60)
\bar{N}_{xy}	$\bar{x} = 0.7, \bar{y} = 0.5$	CSCS/(15/-15)
	$\bar{x} = 0.5, \bar{y} = 0.7$	CSCS/(75/-75) ₅
	$\bar{x} = 0.8, \bar{y} = 0.5$	FCFC/(15/-15) ₅
	$\bar{x} = 0.5, \bar{y} = 0.7$	FCFC/(15/-15)
	$\bar{x} = 0.0, \bar{y} = 0.0$	FSFS/(15/-15)
	$\bar{x} = 1.0, \bar{y} = 1.0$	FSFS/(30/-30)
\bar{M}_x	$\bar{x} = 0.3, \bar{y} = 0.2$	CSCS/(15/-15) ₅
	$\bar{x} = 0.7, \bar{y} = 0.2$	CSCS/(30/-30) ₅
	$\bar{x} = 0.9, \bar{y} = 0.6$	FCFC/(15/-15) ₅
	$\bar{x} = 0.95, \bar{y} = 0.5$	FCFC/(30/-30) ₅
	$\bar{x} = 0.2, \bar{y} = 0.1$	FSFS/(15/-15) ₅
	$\bar{x} = 0.8, \bar{y} = 0.9$	FSFS/(30/-30) ₅
\bar{M}_y	$\bar{x} = 0.8, \bar{y} = 0.9$	CSCS/(75/-75) ₅
	$\bar{x} = 0.8, \bar{y} = 0.9$	CSCS/(60/-60) ₅
	$\bar{x} = 0.0, \bar{y} = 0.3$	FCCF/(60/-60) ₅
	$\bar{x} = 0.0, \bar{y} = 0.5$	FCCF/(75/-75) ₅
	$\bar{x} = 0.05, \bar{y} = 0.7$	FSSF/(60/-60) ₅
	$\bar{x} = 0.0, \bar{y} = 0.3$	FSSF/(75/-75) ₅
\bar{M}_{xy}	$\bar{x} = 0.6, \bar{y} = 0.4$	CSCS/(15/-15) ₅
	$\bar{x} = 0.6, \bar{y} = 0.4$	CSSC/(30/-30) ₅
	$\bar{x} = 0.0, \bar{y} = 0.0$	FCFC/(15/-15) ₅
	$\bar{x} = 0.9, \bar{y} = 0.9$	FCCF/(15/-15) ₅
	$\bar{x} = 1.0, \bar{y} = 0.9$	FSFS/(15/-15) ₅
	$\bar{x} = 0.0, \bar{y} = 0.8$	FSFS/(75/-75) ₅

Table 18: Relative performance matrix considering $CSCS/(15/-15)_2$ and $CSCS/(45/-45)_2$ shells

	Shell actions	$CSCS/(15/-15)_2$	$CSCS/(45/-45)_2$
Positive	\bar{N}_x	1	0
	\bar{N}_y	0	1
	\bar{N}_{xy}	1	1
	\bar{M}_x	1	1
	\bar{M}_y	1	1
	\bar{M}_{xy}	1	1
Negative	\bar{w}	0	1
	\bar{N}_x	1	0
	\bar{N}_y	0	1
	\bar{N}_{xy}	1	1
	\bar{M}_x	1	0
	\bar{M}_y	0	1
	\bar{M}_{xy}	1	1
Total		9	10